RSC Advances



REVIEW

View Article Online
View Journal | View Issue



Cite this: RSC Adv., 2025, 15, 7509

Polymer-based nanocomposites for supercapacitor applications: a review on principles, production and products

The current advances in energy storage devices has necessitated the development of functional polymer-based nanocomposites for supercapacitor applications. Supercapacitors are materials that exhibits enhanced capacitance, power density, life cycle, stability, durability, and catalytic activity. Hence, the incorporation of electrochemically active materials, particularly, carbon-based derivatives can significantly enhances synergistic properties with conducting polymers for advanced applications. Polymer-based derivates are receiving increasing attention and considerations based on their low cost, sustainability, and ease of production in supercapacitor development. Thus, this review highlights the details of the potentials and applications of polymer based nanocomposites from polyaniline (PANI), polypyrrole (PPy), and poly (3,4-ethylenedioxythiophene) (PEDOT) as an advanced materials for supercapacitor.

Received 6th December 2024 Accepted 26th February 2025

DOI: 10.1039/d4ra08601e

rsc.li/rsc-advances

Introduction

One of the key aims of the twenty-first century which is to achieve an energy-sustainable world has necessitated the substitution of conventional fossil fuels with clean, renewable, and green sources. ¹⁻³ Fossil fuels, which are currently the world's primary energy source, are depleting, and growing concerns about anthropogenic emissions of greenhouse gases such as CO₂, which is hastening global climate change and ocean acidification are putting pressure on theirs use to meet our ever-increasing energy needs. ⁴⁻⁶ The hunt for sustainable energy sources has led to the development of novel and improved materials for the design of cost-effective, lightweight, and eco-friendly energy harvesting and storage systems such as (solar cells, batteries, fuel cells, and supercapacitors, among other devices).⁷⁻¹¹ In the design of energy storage devices, there

cules which are molecule commonly created by polymerization

exist three major electrochemical systems; electrochemical

double-layer capacitor (EDLC), battery, and capacitor. Compared to conventional capacitors and batteries, electrochemical double-layer capacitors which are also referred to as supercapacitors are of great interest to researchers due to their excellent performance in generating high energy in the pulsepower state, fast charge, and discharge rates, and long-life cycles.12-18 Recent study have reported that supercapacitors as compared with other energy-storage devices such as batteries, and traditional capacitors each possess robust characteristics that make them suitable for different applications. 19-21 The batteries, such as lithium-ion types, can offer a relatively high energy density typically ranging from 100 to 265 W h kg⁻¹,²² making them suitable for long-term energy storage devices in cases like electric vehicles and mostly portable electronic devices. In contrast, supercapacitors have relatively lower energy densities ranging from approximately 5 to 10 W h kg⁻¹ for electric double-layer capacitors and up to about 50 W h ${
m kg}^{-1}$ for advanced materials making them less suitable for long-term storage devices are of good excellent for applications requiring quick energy bursts. 19,23 However, these unique properties make supercapacitors potential energy storage devices in several applications such as portable electric devices, industrial and power systems, hybrid electric vehicles, electronics, and memory backup systems.20,24 However, the challenges of lower energy density and longer life cycles still need to be addressed.25,26 Carbon materials, conducting polymers, and transition metal oxides are the three (3) groups of electrode materials for supercapacitors.²⁶⁻³¹ Polymers are macromole-

^aDepartment of Metallurgical and Materials Engineering, Federal University of Technology, PMB, 704, Akure, Ondo State, Nigeria

^bMaterials Science and Engineering Program, College of Engineering and Applied Science, University of Colorado, Boulder Co, 80303, USA

^{*}Composites and Advanced Materials Centre, Faculty of Engineering and Applied Sciences, Cranfield University, Bedfordshire MK43 OAL, UK. E-mail: abimbola. orisawayi@cranfield.ac.uk; ao.orisawayi@oaustech.edu.ng; bimboris_t@yahoo.com; Samuel.Taiwo@cranfield.ac.uk

⁴Department of Materials Science and Engineering, Iowa State University, Ames, IA, 50014, USA

^eDepartment of Biomedical Engineering, Federal University of Technology, PMB, 704, Akure, Ondo State, Nigeria

Department of Mechanical Engineering, Olusegun Agagu University of Science and Technology, (OAUSTECH), Okitipupa, Nigeria

of smaller subunits made up of one or more chemical components (monomers) that occur often along a chain.³² "Poly" means "many" and "mer" means "units" in Greek.^{33,34} Polymers composites are becoming prime choices over conventional materials even for essential applications, ranging from everyday household items, electronics, and furniture to high-end applications such as autos, space, aviation, biomedical, energy, and surgical devices due to their extensive utility, low weight, cheap cost, easy processing, and excellent thermal electrical, chemical, mechanical and magnetic properties which can be controlled through the variation of fillers and contents.³⁵⁻³⁷

Polymer composite technological improvements are keeping up with these rising demands as they are termed the materials of the future.38-40 Polymer-based composites with inorganic fillers provide several benefits over single components, including the ability to tune dielectric properties by using fillers with precise physical and chemical properties.41 Dielectric polymer nanocomposites, which have the inherent potential to store energy at the nanoscale level have led to high-performance structures that have a significant influence on long-term goals for more energy-efficient technologies.42-44 For instance, polymer-based dielectric capacitors are widely employed in areas of power transmission, electric vehicles, wind energy generation, radars, and microelectronic systems. 45-50 Conducting polymers has garnered considerable attention from the academic and industrial communities since Heeger, MacDiarmid, and Shirakawa received the Nobel Prize in Chemistry in 2000 for their groundbreaking work on conducting polymer as organic polymers having conjugated double bonds are referred to as conductive polymers. 51-55 Over the years, they have been widely studied for supercapacitors applications owing to their significant high pseudo-capacitance attribute.56-58 They can combine the electrically conductive features of metals or semiconductors with the potentials of typical polymers, such as cheap cost, structural variety, high flexibility, and durability, making them suitable for a wide range of applications in electrochemical devices, supercapacitors, batteries, photovoltaic devices, and sensors.59-63 Polythiophene (PT), poly(3,4ethylenedioxythiophene) (PEDOT), poly(para-phenylene), poly(phenylenevinylene) (PPV), polyfluorene, and polyaniline (PANI) are some of the conducting polymers researched over the years. 64,65 Their composites outperform bulk conducting polymers in terms of energy storage due to their higher conductivity, increased surface area, enhanced electrochemical activity, and excellent mechanical qualities.66 Furthermore, conducting polymer composites offer more benefits resulting from the combined functionality generated from each component because they can effectively be mixed with inorganic materials.67-69 Conducting polymers plays a crucial role in increasing the performance of composites because conducting polymers may interact effectively with inorganic elements to produce a conducting backbone, electrical conductivity, and plastic properties.⁷⁰ Moreover, additive manufacturing technologies have been progressively used in different energy sectors to improve material performance and increase energy efficiency in recent years, and they have been hailed as one of the next-generation options for energy generation, conversion, and storage.³¹ This review highlights the advancements in conductive polymer-based nanocomposites, and the versatile applications in energy storage technologies. It also provides an overview on the relationship between material composition, structure, and properties. The studies on conductive polymers and their composites for supercapacitor applications were reviewed. Furthermore, the review explores potential future directions for enhancing dielectric properties, structural performance, and design flexibility, offering innovative concepts for the development of next-generation supercapacitors, batteries, electrodes, and related technologies.

2. Supercapacitors

Supercapacitors also named electrochemical capacitors or ultracapacitors are devices that store energy with very high capacity and a lower internal resistance than conventional capacitors and provide shorter charging times and longer life cycles than batteries without losing the energy storage capabilities. The mechanism involves the use of energy storage that adopts a simple charge separation that exists at the interface between the electrode and the electrolyte.35,71,72 They are potential candidates for alternative energy storage devices such as batteries and fuel cells due to their high-rate capability, simplicity in principle, reduced maintenance cost, high dynamic of charge propagation, and durability.73 Despite the similarity in their cell construction, supercapacitors can store a significantly higher amount of energy density than conventional capacitors especially when the metal electrodes are replaced by highly porous electrodes.23 A supercapacitor is made up of three essential components which include electrodes, electrolyte, and separator as shown in Fig. 1. The separator isolates the two electrodes electrically. The electrode is used in estimating the capacitance, energy density, and power density of the supercapacitor.74 The electrode is the most essential component of the supercapacitors and it is usually made from materials with high surface area. The specific capacitance can be calculated using eqn (1).

$$C = \frac{Q}{V} \tag{1}$$

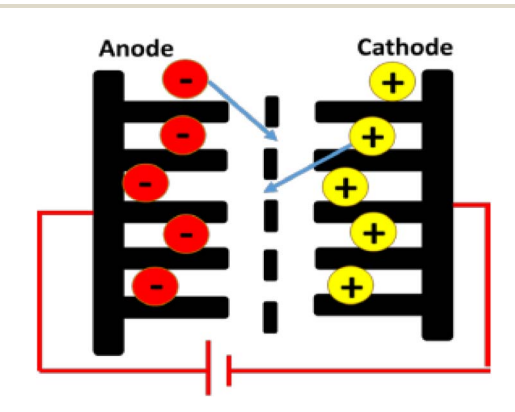


Fig. 1 Major components of a supercapacitor.74

Supercapacitors Double-Layer Capacitors Pseudocapacitors (Helmhotz Layer) (Faradaic charge transfer) Activated carbons Carbon Aerogels Conducting Polymers Metal oxides Hybrid Capacitors Carbon Nanotubes (CNT). Asymmetric electrodes Graphene, Carbide-derived carbon (CDC) Charge storage: Electrostatically and Electrochemically Rechargeable Asymmetric Composite Batterie-type Pseudo/EDLC

Fig. 2 Broad classification of supercapacitors.

where; Q – charged stored on the electrode measured in coulombs (C); V – operating voltage measured in volts (V); C – specific capacitance measured in (F g^{-1}).

Several studies on supercapacitors have focused on fast charge-discharge rates, high power density, and longer life cycles.

2.1 Classification of supercapacitors

Supercapacitors are classified into three based on the energy storage mechanism. ^{75,76} They are classified as;

- (i) Electrochemical double-layer capacitor (EDLC).
- (ii) Pseudocapacitors.
- (iii) Hybrid supercapacitors.

Electric double-layer capacitors (EDLCs) are electrochemical energy storage devices that store energy electrochemically at the exterior part of the electrode-electrolyte interface. It involves a non-faradaic process whereby they store highly reversible charge through electrostatic interactions to promote physical adsorption and desorption of ions at the interface between the electrolyte and electrode with instantaneous forming and relaxing cycles of about 108 s. 70,77 Moreover, during the charging and discharging process, the electrode component does not partake in the chemical reaction. The ion transport, as well as adsorption and desorption of ions, can take place in a few seconds thereby giving EDLSs the ability to charge and discharge faster. They are usually made from electrochemically stable active carbon-based materials such as CNTs and graphenes which have a high surface area. 75 However, factors such as the surface area of the electrode materials, pore structure, and pore size distribution affect the specific capacitance of EDLCs.⁷⁸

Pseudocapacitors store energy based on a fast and highly reversible redox reaction (faradaic process) which occurs on the surface of the electrode or between an electrode and electrolyte. The specific capacitance of pseudocapacitors is usually higher than that of EDLCs made from carbon materials since the reaction takes place both on the surface and in the bulk of the electrode materials.79 However, the major problem associated with pseudocapacitors is the expansion and contraction of the volume of the materials during the charge and discharge process, and this usually results in reduced cyclic stability.80 Several materials including conducting polymers such as polyaniline (PANI), polypyrrole (PPy), and some metal oxides have been studied as materials for pseudocapacitors. Pseudocapacitors store energy in devices through the combination of both pseudocapacitance and the electric double-layer capacitance provided by the surface of the active material.81 The hybrid (symmetric or asymmetric) supercapacitors adopt the use of a variety of electrode materials with enhanced capacitance, higher operating voltage, and energy density. They are designed to mitigate the challenges of reduced capacitance, high resistivity, and yield loss attributed to the poor cyclability of metal oxide and hydroxides.76 Fig. 2 shows the broad classification of supercapacitors while Table 1 presents the differences between EDLCs and pseudocapacitors.

Table 1 Difference between EDLCs and pseudocapacitors

EDLC	Pseudocapacitors
Non-faradaic does not involve redox reaction A double layer is formed at the interface	Faradaic, involves a redox reaction No double-layer formation
Good cyclic stability Good power performance No mechanism failure	Higher specific capacitance Higher energy density This always depends on the redox reaction

3. Functional polymers for supercapacitors application

Nowadays, the use of polymers for supercapacitor applications has garnered wide attention due to their unique properties such as flexibility, lightweight, and stable cycling capabilities. Moreover, redox-active polymers possessing good recyclability and sustainability are better and safer substitutes for heavy metals in battery electrodes.82 The gross demand of industries for highly sustainable future-generation electronics has led to the revolution of concerted efforts for the designs of cost-effective, lightweight, eco-friendly, and high-performance supercapacitors and batteries.83 Besides, the current search for sustainable energy has increasingly become a leading position as one of the most important global concerns due to the uptrend in the depletion of fossil fuels.84 Hence, there is a need for research to discover more suitable and sustainable materials for energy applications globally in which polymer has been highly considered. Among the polymers, conducting polymers have been discovered to be a group of organic polymers capable of conducting electricity due to the presence of delocalized molecular orbitals in them, and may also be used as semiconductors. They developed about 20 years ago and gained a lot of interest over the years due to their economic importance, electrical conductivity, appreciable environmental stability, and mechanical, optical, and electronic properties.85 In general, conducting polymers exhibit different structures in combination with higher specific capacitance as

shown in Fig. 3 and Table 2 which make them good materials for the development of new-generation energy storage and devices. S6,87 Conducting polymers are broadly classified into three major groups as;

- (i) Ionic conducting polymers.88
- (ii) Intrinsically conducting polymers (ICPs).89
- (iii) Conducting polymer composites.90

The mechanisms by which conducting polymers are being used for supercapacitors in based on the fact that they have a π conjugated backbone which comprises a regularly alternating single (C-C) and conjugated (C=C) bonds.91 The generation and propagation of charger carriers arise from the π -conjugated backbone while the charge storage in conducting polymers is attributed to ionic mobility that occurs under redox processes over a range of potentials when oxidation takes place, ions are transported to the polymer backbone, and when reduction occurs, the ions are released back into the solution, and this gives room for the achievement of high capacitance ratio.^{29,91} Polymer-based supercapacitors utilize a reversible electrochemical doping process for charge storage. A quasi-rectangular cyclic voltammogram often indicates this process, which may exhibit reversible redox peaks linked to a battery-like reaction. During charging and discharging, the polymer undergoes reduction with cation insertion from the electrolyte (n-doping) or oxidation with anion insertion (p-doping). This leads to the formation of delocalized charge carriers along the polymer chains.92,93

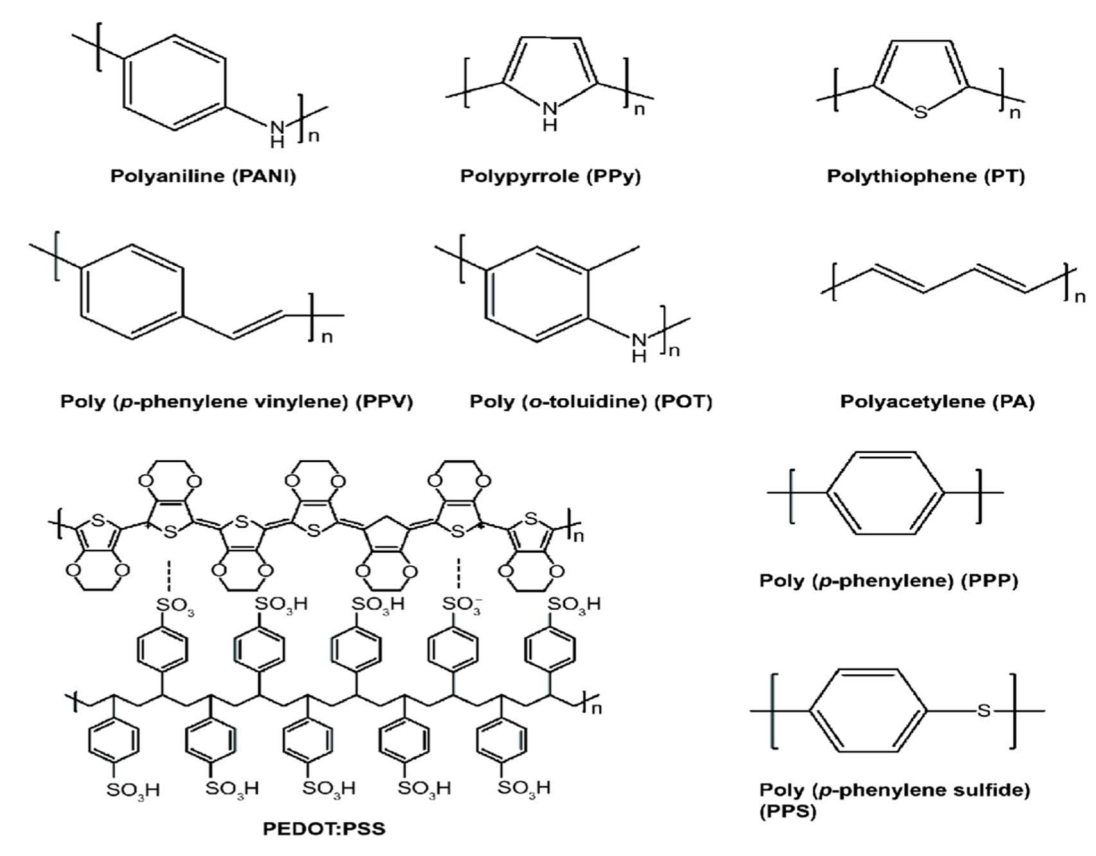


Fig. 3 Chemical structures of selected conducting polymers. 101

Table 2 Conductivities of certain conducting polymers^a

tors n, p	20, 200
	30-200
p	10-7500
-	0.4-400
-	0.4-400
	200-1000
-	500
	3-300
p	1-1000
p	1-50
	p n, p p n, p p

However, the transport and release of charged ions which causes expansion and contraction of conductive polymers under the action of ions and charges often leads to the degradation of the cycle stability,94 self-discharging, and poor efficiency in overall capacities.95 To mitigate these problems, the design of composites comprising conductive polymers and other materials such as carbon fiber, carbon black, carbon nanotubes96,97 or graphene76,98 has been devised as a feasible remedy. These composites offer more benefits resulting from the combined functionality generated by each component. The effective mixing of inorganic materials with conducting polymers plays a crucial role in increasing the performance of composites because conducting polymers may interact effectively with inorganic elements to produce a conducting backbone, electrical conductivity, and plastic properties. 67,99,100 The cycle stability of these composites' electrodes can be improved by enhancing the molecule chain, segment structure, mechanical stability, electroconductibility, and machinability to eradicate the issues associated with mechanical stress.

In this review, polyaniline (PANI), polypyrrole (PPY), polythiophene (PT), and poly(3,4-ethylenedioxythiophene) (PEDOT) are selected and discussed.

3.1 Polyaniline

Polyaniline (PANI) has gained significant attention among CPs since it was first synthesized in 1886, due to its excellent electrochemical properties, good conductivity, and its high theoretical capacity at various redox states. ¹⁰² It can be used either as a conductive agent or used directly as electrode material in energy storage devices owing to its tailorable pseudocapacitive performance which is based on its variety of oxidation states. ⁸⁴ Moreover, its unique properties such as high conductivity, excellent redox reversibility, environmental stability, unvarying conduction principles, rapid faradaic reactivity, excellent resistance to the effects of oxygen and water, and ease of synthesis *via* different processing routes make PANI a potential material for practical applications. ^{90,103,104}

Polymer-based nanocomposites, such as polyaniline (PANI), offer numerous advantages, including high electrical conductivity, ¹⁰⁵ easy synthesis, ¹⁰⁶ excellent environmental stability, ¹⁰⁷ and tunable properties through doping. ^{105,108} They are cost-

effective and exhibit outstanding mechanical strength when combined with other materials. Thanks to their unique electrical and chemical properties, PANI-based nanocomposites are highly versatile and find applications in sensors, anti-corrosion coatings, energy storage devices, and many other fields. ^{105,109-111} Apart from the above mentioned advantages, compared to ther composites the other advantages of PANI includes lightweight nature and large surface area which improves performance applications like adsorption and sensing. ¹¹²

Although PANI-based nanocomposites may not have the high mechanical strength of carbon fiber composites, they are more affordable and have better electrical conductivity. PANI composites are also more flexible and lighter than metal-based composites while yet having superior electrical conductivity. Processing difficulties, such as obtaining homogeneous dispersion of nanoparticles inside the polymer matrix, are crucial factors to take into account, since they may affect the final qualities. Furthermore, depending on the particular application, reinforcing fillers may be needed to increase the mechanical strength of PANI composites.

Conducting PANI can be produced from the electrodeposition of aniline monomer either through chemical oxidative polymerization or direct electrochemical polymerization in the presence of an oxidizing agent and a doping material. 117,118 Besides, both synthesis methods adopted and the level of kind of dopants used have significant effects on the electrochemical potential and electrical conductivity of PANI.119 Likewise, interfacial polymerization, electrospinning, seeding polymerization, and templated polymerization have also played important roles in the preparation of PANI. 120 Though the theoretical specific capacitance of PANI is estimated to be around 2000 F g^{-1} , experimental values are much lower since the percentage of effective PANI depends on the conductivity of PANI and the diffusion of counter-anions. 121,122 Synthesized PANI powder through chemical solution polymerization and carried out galvanostatic charge-discharge (GCD) and cyclic voltammetry tests to evaluate the electrochemical properties of PANI single electrode in 1 M HCl and 1 M H2SO4 electrolyte solutions. It was found that the specific capacitance of the single PANI electrode is 302.43 F g^{-1} . More so, interfacial polymerization was adopted by Sivakkumar et al.123 to synthesize PANI nanofibers and the

developed redox supercapacitor consists of a two-electrode cell having an initial specific capacitance of 554 F g⁻¹ at 1.0 A g⁻¹ but rapidly decreases under continuous cycling. It is regarded as the cheapest and the most thermally stable intrinsically conductive polymer and, due to all these merits it offers, the design of PANI as a pseudocapacitor material has gained a lot of interest in terms of research for supercapacitors application.⁷⁸ However, despite its high capacitance value owing to its multiple redox states which might also lead to a large surface potential during charging and discharging while transferring from one oxidation state to another, PANI does swell, shrink, or even degrade during the long cycle of charging and discharging. This is caused by the structural damage of the main chain and results in poor conductivity and stability.⁵⁶ Effective remediation to these problems is by incorporating carbon nanomaterials. PANI with ordered nanostructures does possess high specific surface area, excellent cycle stability, high energy storage capacity as well as excellent performance rate in comparison to randomly connected geometries. 103,124,125 Also, the synergy of designing a composite comprising PANI and various active materials, especially carbon materials has been at the forefront of research to enhance the conductivity, stability of I, and the specific capacitance of PANI towards achieving high electrochemical performance. Several functional carbon materials have been incorporated into PANI nanostructured composite to adequately improve their electrical and mechanical stability to produce a high pseudo-capacitance PANI.

Xu *et al.*, ¹²⁶ prepared zinc sulfide and reduced graphene oxide (ZnS/RGO) *via* hydrothermal technique and doped conductive polymers (PANI, PPy, PTh, and PEDOT) of the same mass ratio (70 wt%) using *in situ* polymerization on the surface of the ZnS/RGO composite. The experiments show that for supercapacitor applications, the ZnS/RGO/PANI ternary electrode composite has the best capacitance performance and cycle stability compared to all other polymer-doped ZnS/RGO composites in which the three-electrode system, the ZnS/RGO/PANI has a discharge specific capacitance 1045.3 F g⁻¹ and cycle stability of 160% at 1 A g⁻¹ after 1000 loops. It was discovered that the composite has a discharge-specific capacitance and cycle stability of 722.0 F g⁻¹ and 76.1% at 1 A g⁻¹ and

the greatest energy and power density of $349.7~W~h~kg^{-1}$ and $18~kW~kg^{-1}$ in a two-electrode symmetric system. The authors concluded that conductive polymers can efficiently enhance the voltage range of electrode composite for the two-electrode system, thus making them promising electrode materials for supercapacitors.

Adopting a viable *in situ* chemical oxidative polymerization technique, Devadas and Imae¹²⁷ synthesize polymer/carbon dot composites and investigated the effect of carbon dots on the specific capacitance of conducting polymers using PANI and PPy. The polymer/Cdot composites exhibited enhanced specific capacitance and long-term stabilities due to the combined effect of polymers and the C-dots. However, the incorporation of the Cdots into the composites doubled the capacitance of the original polymers. The specific capacitances of the composites were estimated to be 676 and 529 F g⁻¹ for PPy/Cdots and PANI/Cdots, respectively at a current density of 1 A g⁻¹ and the work reports excellent capacitance retention and satisfactory durability reinforcement of pseudocapacitors by the simple addition of less-conductive carbon material.

Shanmugavadivel et al.128 synthesized an electro-active inorganic-organic nanohybrid PANI-composite via surfactantassisted chemical polymerization reaction of aniline with nanocrystalline BaMnO3. The results of the electrochemical studies carried out using cyclic voltammetry and galvanostatic charge-discharge measurements as shown in Fig. 4 showed that the improvement in the properties of the electrode emanates from the synergistic influence of PANI and BaMnO₃. Fig. 4a reveals the XRD patterns of PANI/BaMnO₃ nanohybrid in which the sharp and intense peaks indicate the high degree of crystallinity of polyaniline through the addition of nanocrystalline BaMnO₃. A reduction in the intensity of diffraction peaks was noticed in the PANI-BaMnO₃ hybrid nanocomposite compared to pure BaMnO3, which indicates that the amorphous nature of PANI has changed into crystalline form due to the presence of the hexagonal BaMnO₃ incorporated in the PANI matrix while Fig. 4b. FT-IR spectrum of PANI-BaMnO₃ affirm that the spectrum formed contains contributions from PANI and BaMnO3. The hybrid composites exhibited a high specific capacitance, energy density, and power density of 560.5 F g^{-1} ,

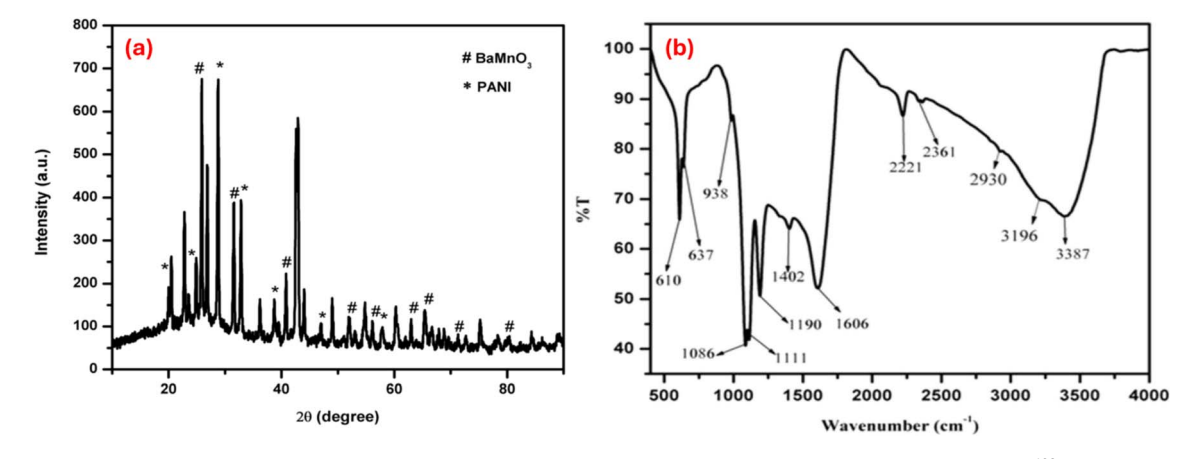


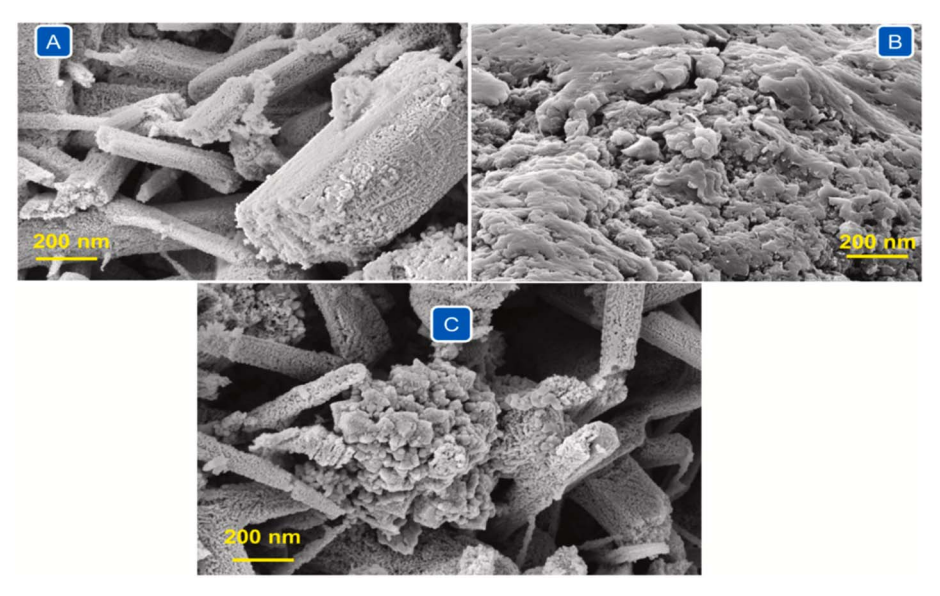
Fig. 4 (a) XRD patterns of PANI-BaMnO₃ nanocomposite and (b) FT-IR spectrum of PANI-BaMnO₃ nanocomposite.¹²⁸

32.01 W h kg⁻¹, and 400 kW kg⁻¹ respectively, and also have excellent stability and cycling performance with less than 5% loss in capacity over under 500 cycles.

Lee et al.129 produced chemically activated multiwalled carbon nanotubes polyaniline composites (PANI/A-MWCNT) using the ultrasonic polymerization technique and investigated the composites as suitable electrode materials for supercapacitors. The comparison of this composite to pristine MWCNTs shows that the effect of pore structures developed due to the polymerization process could adequately foster the homogenous dispersion of aniline and invariably result in excellent cycling performance. More so, the authors concluded that the interaction between the conjugated structure of carbon and the PANI quinoid ring resulted in the charge transfer enhancement. Kathalingam et al. 130 studied the structural and electrochemical attributes of PANI-incorporated ZnCO2O4@N-GO hybrid nanocomposite developed by thermal reduction. The ZnCO₂O₄@N-GO/PANI nanocomposite possesses enhanced porosity and electrochemical properties. Moreover, the SEM and TEM analysis of the composites shows that ZnCO₂O₄@N-GO and ZnCO2O4@N-GO/PANI have spherical and plateshaped particulates, respectively affirming the effects of PANI in forming flakey shapes. The PANI-reinforced electrode shows excellent electrochemical properties, enhanced porosity, conductivity, and catalytic performance with good cyclic stability (specific capacitance of about 720 F g⁻¹ and 96.4% retention after 10 000 cycles in 3 M KOH) which is significantly superior to ZnCO₂O₄@N-GO composite. Hence, the developed PANI-incorporated composite is recommended as a promising catalytic material for supercapacitor applications. Having identified that slow redox reaction rate and poor conductivity have limited the applications of manganese oxide despite its low cost and high specific capacitance, Zhuang et al., 131 developed a novel composite in which nanoparticle Mn₃O₄ is doped on activated carbon through a thin conductive polyaniline layer

as a coupling agent. This PANI layer having crosslinked networks exhibits good electrical conductivity and the interface is highly compatible with anchoring the nanoparticle Mn₃O₄ which also has an interconnected porous structure with enough ion migration channels and a large surface area. The novel composites exhibit a high specific capacitance of 325 F g⁻¹ at 0.5 A g^{-1} and excellent performance rate of 248 F g⁻¹ at 20 A g⁻¹ and remarkable cycle stability of 90% retention after 10 000 cycles. The authors concluded that the developed asymmetric supercapacitor exhibiting a high energy density of 33.8 W h kg $^{-1}$ has a good prospect of finding application in the electrochemical energy storage fields. In another work, Rajkumar et al.132 synthesized FeCo2O4/PANI via in situ polymerization techniques and characterized it using various physicochemical methods to ascertain its applicability as an electrode in supercapacitors. The characterization of the asprepared FeCo₂O₄/PANI composites possesses a high specific capacitance of 940 F g^{-1} at the current density of 1 A g^{-1} . The enhanced capacitance is attributed to the porous nanorod-like structure with a relatively high number of active sites as shown in Fig. 5. This significantly resulted in good ion and electron transport and makes the produced composites a potential material for electrode materials in advanced energy storage devices, thereby combining the cost-effectiveness, ecofriendliness, abundance, and rich redox reaction advantages of both iron and cobalt cations.

Ma et al. 133 prepared short cluster shape graphene oxide/ polyaniline/metal hydroxide (GO/PANI/metal hydroxide) nanocomposite via one-step in situ polymerization and added nickel and cobalt ions. The content of Ni2+ and Co2+ in the nanocomposite was easily tuned by altering the mass ratio of the metal salts in the reactions. The electrochemical analysis revealed that GO/PANI/metal hydroxide doped with only Ni²⁺ had the highest specific capacitance of 743 F g⁻¹ compared to the other that was doped with Co²⁺ and the value was stable



FESEM image of (A) FeCo₂O₄ (B) PANI and (C) FeCo₂O₄/PANI. 132

with a capacitance reduction of 15.6% after 2000 cycles. The experimental results also affirmed that the shape tunable GO/ PANI/Ni(OH)₂ nanocomposites will be an excellent electrode material in supercapacitors. In another study, Srinivasan et al., 134 adopted various physicochemical techniques in confirming the formation of as-synthesized BiVO₄/PANI prepared by in situ polymerization technique. The authors studied the electrochemical performance of the BiVO₄/PANI composite as a potential electrode material for electrochemical energy storage applications using cyclic voltammetry (CV), galvanostatic charge-discharge (GCD), and electrochemical impedance spectroscopic (EIS) techniques. It was observed that the specific capacitance of the BiVO₄/PANI composite was estimated to be 701 F g^{-1} at the current density of 1 A g^{-1} and exhibited 95.4% retention of the original capacitance after 5000 cycles. Palsaniva et al. 135 adopted the in situ polymerization technique in fabricating symmetric tandem supercapacitors (STC) using PANI/ RGO/ZnO nanocomposite. The polymerization method helps to ensure the formation of a homogenously mixed nanocomposite. The author reported that the morphological analysis of the nanocomposites shows that the PANI/RGO/ZnO with a ratio of 2:1 (PANI: ZnO) has a higher surface area which invariably contributes to excellent ionic diffusion and resulted in a high specific capacitance of 40 F g⁻¹ at a current density of 0.05 A g⁻¹. The as-prepared symmetric supercapacitor device shows excellent electrochemical performance and high capacitance retention of 86% after 5000 cycles and exhibited specific energy of 561 W h kg⁻¹ and specific power of about 403 W h kg⁻¹. These unique properties can be attributed to the synergic influence of ZnO, PANI, and RGO in the 2:1 nanocomposite. The potential and importance of graphene oxide in the development of high-performance energy storage systems which are based on polyaniline were demonstrated by Mitchell et al. 136 when the authors deposited multilayer films of PANI

and graphene oxide on indium tin oxide (ITO) electrodes. They reported from the study that the multilayer film has an enhanced specific capacitance compared to virgin polyaniline film. Specific capacitances of 201 F g^{-1} and 429 F g^{-1} were achieved for PANI and PANI/GO multilayer electrodes, respectively. These improvements in the electrochemical performances of the multilayered PANI/GO electrode were explained to be due to the increase in the number of active sites for the deposition of polyaniline provided by the large surface area of the graphene oxide sheets and the combined effect of the polyaniline and graphene oxide. Also, the beneficial role of protic ionic liquid PIL in synthesizing PANI and PANI/GO nanocomposites with excellent supercapacitance performance was demonstrated by Al-Zohbi et al. (2021).137 In this study, the oxidative polymerization technique was used in synthesizing PANI in a mixture of water and pyrrolidinium hydrogen sulfate [Pyrr][HSO₄]. A comparison of the PANI/PIL with convectional PANI shows that the addition of PIL to the polymerization medium causes the change in the morphology to fiber-like instead of spherical-like morphology. More so, the PANI/PIL shows improvements in charge transfer kinetic and storage capability. The addition of 16 wt% GO to the PANI/PIL optimized the weight ratio of the nanocomposite and resulted in a material that exhibited the best performance and stability of 223 F g^{-1} at 10 A g^{-1} , 4.9 W h kg^{-1} and 3700 W kg^{-1} at 10 A g^{-1} . Fig. 6 displays the schematic diagram of the preparation of the route of the tetragonal prism array of TiO2 deposited on fluorine-doped tin oxide (FTO) prepared by hydrothermal reaction before depositing PANI coating on it. This was proven to be an efficient electrode material for supercapacitors as the electrode consisting of PANI/TiO2/FTO composite exhibited a specific capacitance of 78 F g^{-1} at a current density of 1 A g^{-1} by Chen et al.138 This is similar to Ur Rahman and his coworkers, 117 work where they surface-modified fluorine-doped tin

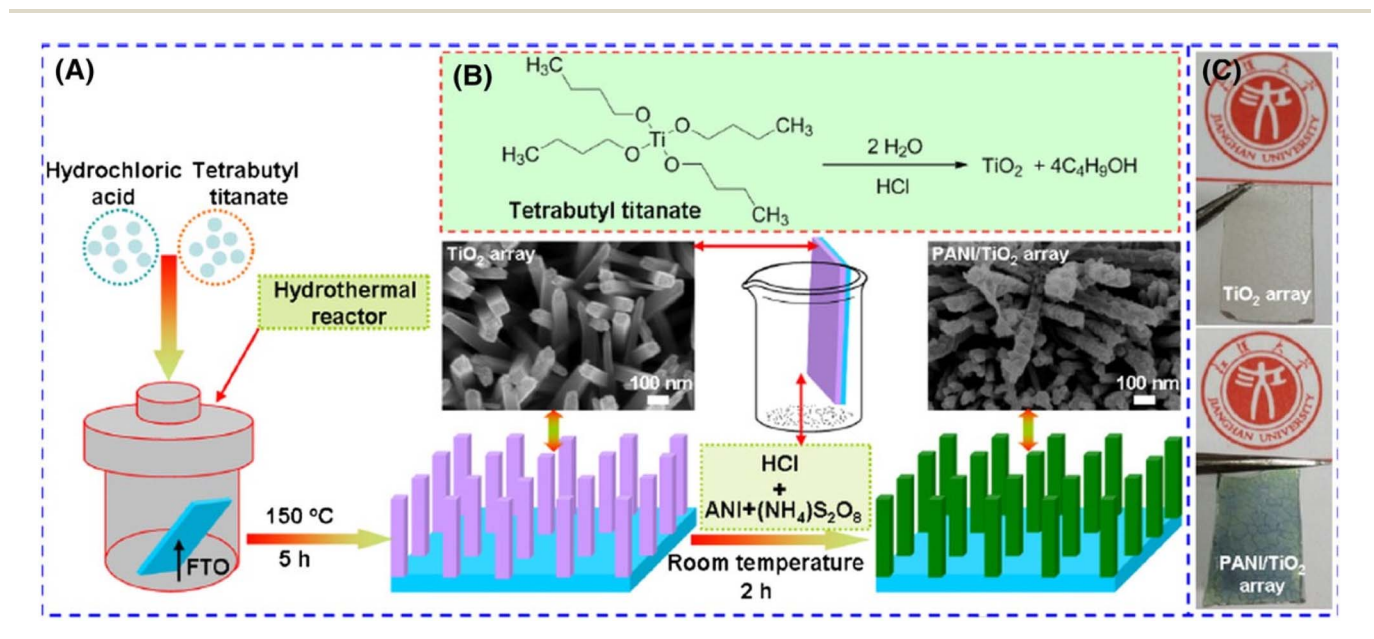


Fig. 6 (A) Synthesis of tetragonal prism array of TiO_2 deposited on fluorine-doped tin oxide (FTO) and followed by PANI coating, (B) synthesis of TiO_2 array *via* hydrolysis process, and (C) optical images of TiO_2 /FTO and PANI/ TiO_2 /FTO.¹³⁸

Review **RSC Advances**

oxide (FTO) with sodium phytate-doped PANI in the absence of binder and to examine its suitability as a novel current collector in symmetric supercapacitor devices. The authors constructed a symmetrical cell configuration with binder-free electrodes. The device exhibited excellent electrochemical performance with high specific capacities of 550 F g^{-1} at 1 A g^{-1} , 355 F g^{-1} at 40 A g⁻¹, and excellent cycling stability of 90% retention of the initial capacity over 1000 charge/discharge cycles. Furthermore, the supercapacitor has a remarkably high power density of 73.8 W h kg⁻¹ at 500 W kg⁻¹.117

A schematic of the synthesis procedure of rGO/TiO2/PANI nanocomposite is shown in Fig. 7. The nanocomposite was synthesized using varying initial feed ratios of rGO; TiO2 aniline monomer in the ratio of 1:5:1, 1:5:2, 1:5:3, 1:5:4, 1:5:5. The result of the electrochemical performance analysis of the rGO/TiO₂/PANI nanocomposite confirm that the nanocomposite exhibited better performance than individual constituents in terms of specific capacitance, energy density,

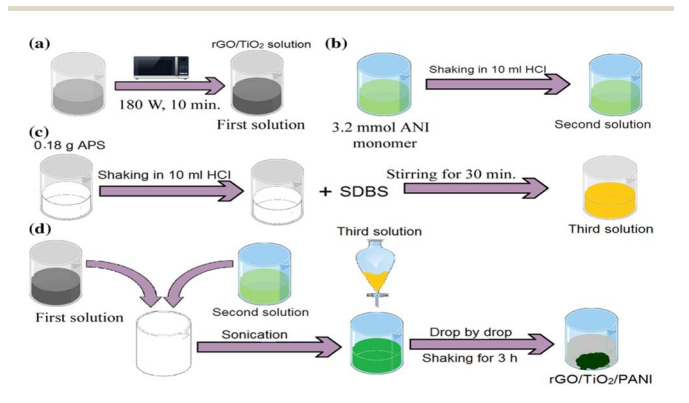
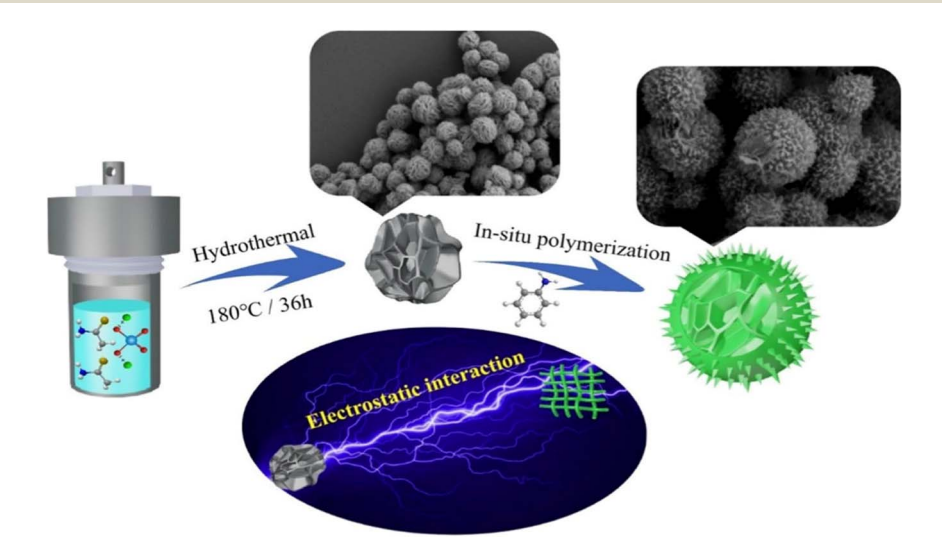


Fig. 7 Schematic showing the synthesis of rGO/TiO₂/PANI nanocomposite via in situ emulsion polymerization: (a) preparation of rGO/ TiO₂ suspension, (b) addition of 3.2 mmol ANI monomer, (c) addition of 0.18 g APS and SDBS with stirring and (d) sonication drop-by-drop addition of APS solution with shaking for 3 hours. 139

power density and stability retention with the rGO: TiO2: PANI in ratio 1:5:4 having the highest specific capacitance of 692.87 F g⁻¹. Also, using a novel real circuit model, the developed device was able to power a LED lamp (1.8 V) for 180 seconds which implies the rGO/TiO₂/PANI nanocomposite may be used as a potential material for cost-effective and eco-friendly energy storage systems.139

Another ternary composite comprising PTP/PANI/TiO2 was synthesized by Thakur et al.140 The work involves the mixing of two polymers; polyaniline and polythiophene, followed by adding TiO2 particles which is transition metal oxide with variable oxidation state to the blended polymer matrix. The PTP/PANI/TiO₂ ternary composite shows improved capacitive performance (specific capacitance of 265 F g⁻¹ and energy density of 9.09 W h kg^{-1} at 1 A g^{-1}) compared to its components in pristine form. Chen et al. 141 improved the cyclic stability of PANI by adding urchin-like molybdenum disulfide (MoS₂) to PANI as a hybrid electrode material through in situ oxidative polymerization as shown in Fig. 8. From Fig. 9, it can be observed from the SEM that, the pure MoS₂ in Fig. 9a a had a flower-like morphology consisting of a sheet-like petal which provides more active sites for the countless branches of the dendritic polyaniline macromolecular chain as shown in Fig. 9b while Fig. 9c-g show the changes in the morphology of the MoS₂/PANI composite with an increase the loading fraction of MoS₂ which is why Fig. 9c exhibits a combination of dendritic structures and PANI and flower-like spheres of MoS₂. Thus, a sea urchin structure was observed in the hybrid composite with an increase in MoS2 content while the dendritic structure of the PANI disappears gradually in Fig. 9d-g. The electrostatic bond and hydrogen bond relationship between MoS2 and PANI causes improvement in the structural integrity and specific surface area of the hybrid electrode materials. Especially the MoS₂/PANI reinforced with 25 wt% of MoS₂ (PM₂₅) has the best combination of properties as it exhibits a maximum capacitance of 645 F g⁻¹ at 0.5 A g⁻¹ with excellent cycling stability of 89% capacitance retention after 2000 cycles at a current density



An illustration of the synthesis process of MoS₂/PANI hybrids through in situ oxidative polymerization.¹⁴¹

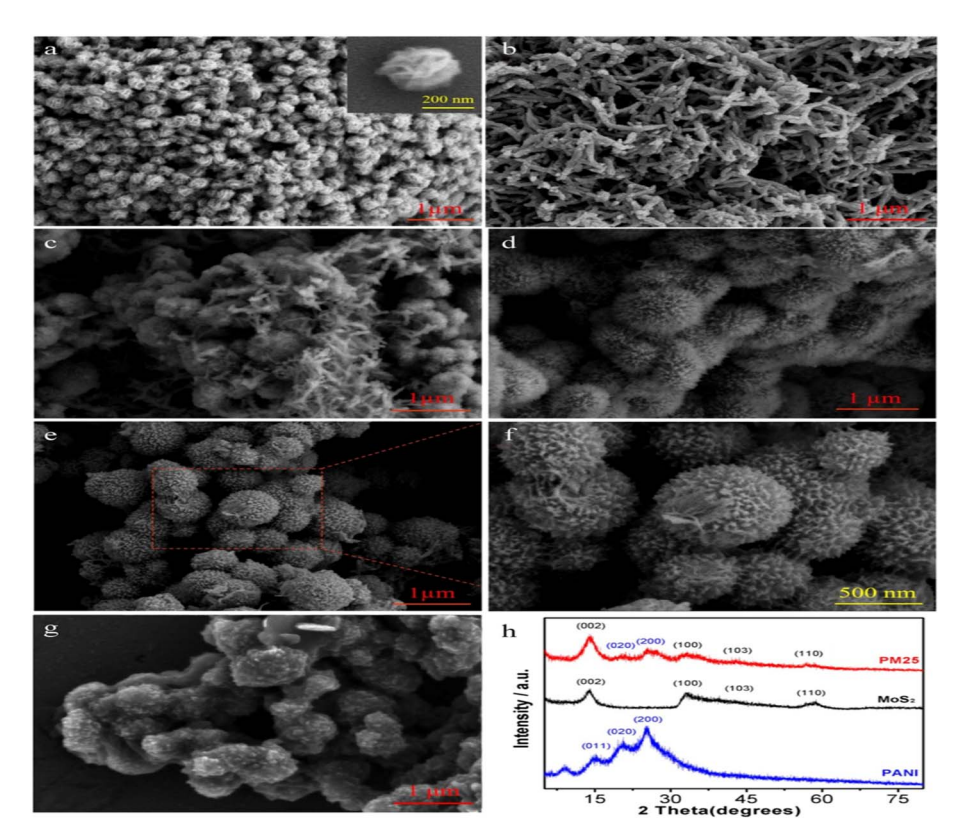


Fig. 9 SEM images of (a) pure MoS₂, (b) pure PANI; (c) PM₁₅; (d) PM₂₀; (e) and (f) PM₂₅; (g) PM₃₃; and (h) XRD patterns of PANI, MoS₂, and PM₂₅. ¹⁴¹

of 10 A $\rm g^{-1}$. In comparison to virgin PANI (335 F $\rm g^{-1}$), the enhancement in the electrochemical properties affirms that urchin-like MoS₂/PANI hybrid electrode materials with stable and unique morphology are promising materials for hybrid supercapacitors applications.

Interdigitated and sandwich electrodes based on reduced graphene/polyaniline nanocomposite were prepared using a simple, eco-friendly, degradable and sizeable approach as shown in Fig. 10. The nanocomposite was fabricated using a hydrothermal method and drop-casted directly on the poly(ethylene terephthalate) (PET) substrate to form supercapacitor electrodes. No mechanical press was used in the process as active materials have excellent adhesion to the substrate. The capacitance of the developed supercapacitor was estimated to be 99 F g⁻¹ at a 0.5 mA current and exhibited good capacitance retention above 98.3% after 1000 cycles. The as-prepared sandwich supercapacitors have a low charge transfer resistance of 1.75 ohms and obtained capacitance retention of 83% even when the current density varied from 0.25 to 5.0 A g^{-1} . This shows the potential of the developed nanocomposites for hightech supercapacitor applications in future electronic devices. 142

Hosseini et al., 143 prepared Fe $_3$ O $_4$ nanoparticles on chitosangraphene oxide multiwalled CNTs before grafting PANI on it using in situ chemical polymerization. The investigation of the capacitive properties of the as-prepared electrode in a three-electrode configuration in 0.5 M Na $_2$ O $_4$ electrolyte through several electrochemical techniques shows that the specific

capacitance of the CS/GM/Fe₃O₄/PANI electrode is estimated to be 1513.4 F g^{-1} at 4 A g^{-1} which is about 1.9 times greater than that of CS/GM/Fe₃O₄. More so, the electrode has a life cycle of 99.8% specific capacitance retention at 100 A g^{-1} . The combined influence of chitosan/graphene oxide multiwalled CNTs coupled with the excellent properties of PANI has made the nanocomposite a potential material for supercapacitor applications. In another work, a new PANI/Co3O4 supercapacitor electrode with great potential for high-performance energy storage devices was prepared by hydrothermal and in situ polymerization techniques using foamed nickel as substrate. The evaluation of the PANI/Co₃O₄ by XRD, SEM, TEM, and XPS reveals that the Co₃O₄ nanorods were uniformly coated with PANI. However, the electrochemical investigation shows that the specific capacitance of the PANI/Co₃O₄ nanocomposite is 3105.46 at 1 A g^{-1} which is about 14.7 times greater than that of Co₃O₄. It was also discovered that the composite has satisfactory capacity retention of 74.81% after 3000 cycles and a very high energy density of 58.84 W h kg⁻¹ at 0.16 kW kg⁻¹.144 Yu et al.122 also prepared PANI/G-MS composite using sheet-like polyaniline and graphene oxide as starting material and adopted spray-drying and chemical reduction processes in the preparation. They confirmed that uniformly coated PANI on the surface of graphene tends to provide high conductive networks which fasten electronic transport in the composite for supercapacitors. Additionally, the composite form many channels within the spherical particles during the random stacking of the

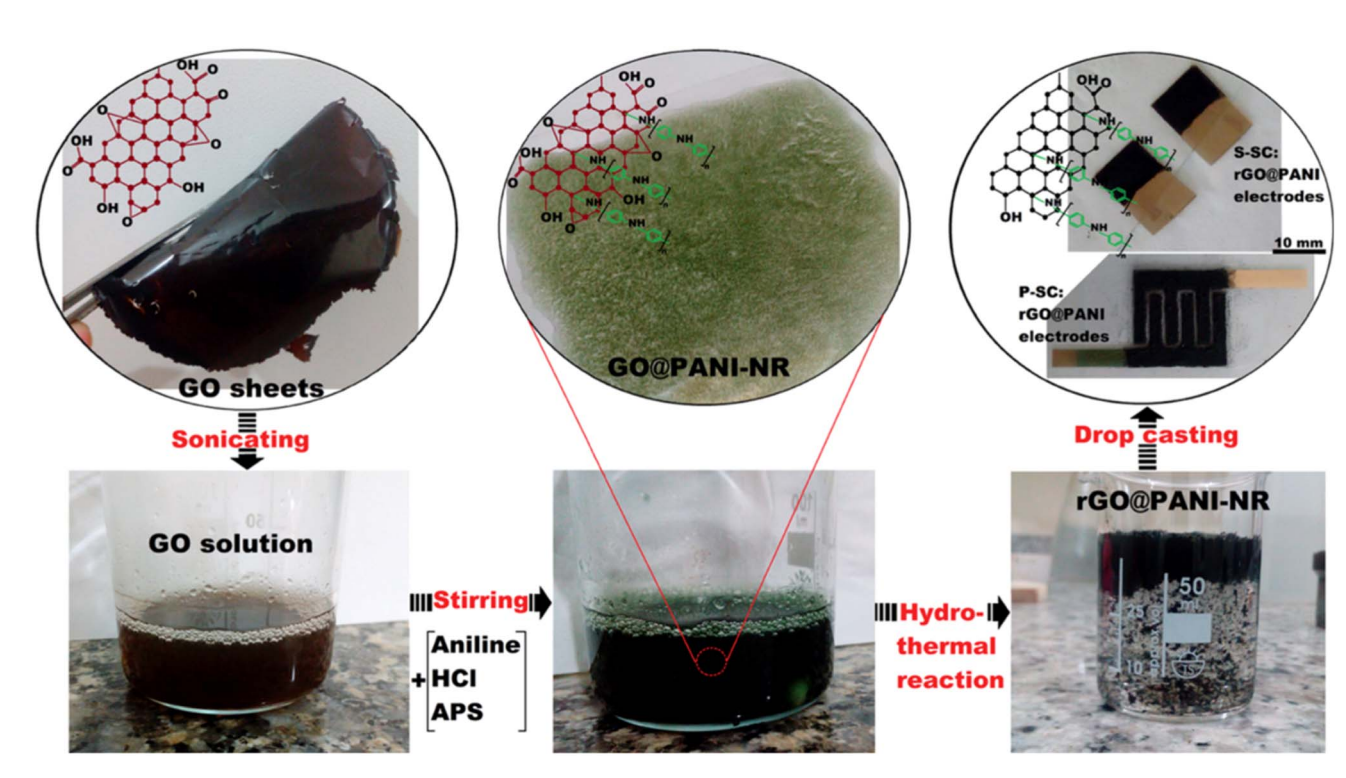


Fig. 10 Image showing the simple and ecofriendly synthesis and development procedures for rGO/PANI nanocomposites as active materials and supercapacitor electrodes.¹⁴²

sheet-like PANI/GO composite through the spry-drying process. The emergence of a unique structure enhances the electrochemical capacitance of the as-prepared PANI/G-MS composite to 596.2 F g^{-1} at 0.5 A g^{-1} , 447.5 F g^{-1} at 20 A g^{-1} , and retained 83.7% of the initial capacitance after 1500 cycles. Carbon nanoonions (CNO) were successfully integrated into PANI by Majumder et al.145 via in situ oxidative polymerization of the aniline monomer. This invariably led to the overall improvement in the electrochemical properties of PANI. The PANI/CNO composite with hybrid heterostructure shows good specific capacitance of 196 F g⁻¹ at the current density of 1 A g⁻¹ and enhances energy and power densities. CNO improves the electronic conductivity, reduces the PANI fiber agglomeration rate, and initiates a larger active surface for the existence of electrolytic ion interactions. Concurrently, the combined effect of CNO and the PANI causes the co-existence of both electric double layer and pseudocapacitive specific capacitance in the nanocomposite while the mesoporous morphology gives room for ultrafast ion diffusion route for both electrolytic ions and the electrons. Ji et al. 146 developed a bio-inspired micro-nanohierarchical rGO/BPANI composite via photolithography, colloidal lithography, and soft-template techniques. The surface area of the electrode/electrolyte interface of the PANI electrode was increased due to the bio-inspired micro/nano artificial structure, thus improving the ion-electrolyte transport. Moreover, the addition of rGO enhanced the total EDLC and PC performance of the bioinspired PANI composite and thereby, caused enhanced electrochemical conductivity, reduced internal resistance, and increased life cycle. The capacitance properties increased to 614 F g⁻¹ at 1.0 A g⁻¹ and

satisfactory stability of 85% after 10 000 cycles at 5.0 A g⁻¹. This fabricated bio-inspired template exhibited excellent flexibility and mechanical attributes and showed stable performance under cycling for 2000 cycles at 5 mV s⁻¹ with no defect in the electrochemical performance. Hence, this novel bio-inspired micro/nanoarchitecture was affirmed to possess special properties for electrochemical energy storage in flexible devices. Heydari et al.147 studied the electrochemical behavior of ternary PANI/MoS₂-MnO₂ for supercapacitor applications. In this work, bulk MoS2 was exfoliated into layered nanosheets with a unique solvent. Thereafter, MoS2-MnO2 composite was prepared by hydrothermal technique and hybrid PANI/MoS2-MnO2 composite was synthesized via electro-polymerization method. The processes involved in the synthesis of this ternary hybrid composite are shown in Fig. 11. Each of the components serves specific purposes, MoS2 provides sub-layer supports and MnO2 enhances the electrochemical performance while PANI improves the electric conductivity of the hybrid composite. Analysis of the hybrid composite using various techniques shows that the maximum specific capacitance of PANI, MoS₂-MnO₂, and PANI/MoS₂-MnO₂ measured at a scan rate of 5 mV s⁻¹ was 333, 358, and 479 F g⁻¹, respectively. Likewise, the designed two-electrode device made from the composition of PANI/MoS₂-MnO₂ with a larger porous structure exhibits a specific capacitance of 259 F g^{-1} at a current density of 1 A g^{-1} , specific energy density of 35.97 W h kg⁻¹ at a specific power of $500~\mathrm{W~kg^{-1}}$ and satisfactory cycling stability of 94.1% after 4000 cycles at 16 A g⁻¹. Table 3 presents the electrochemical performance of various supercapacitors fabricated based on polyaniline electroactive materials.

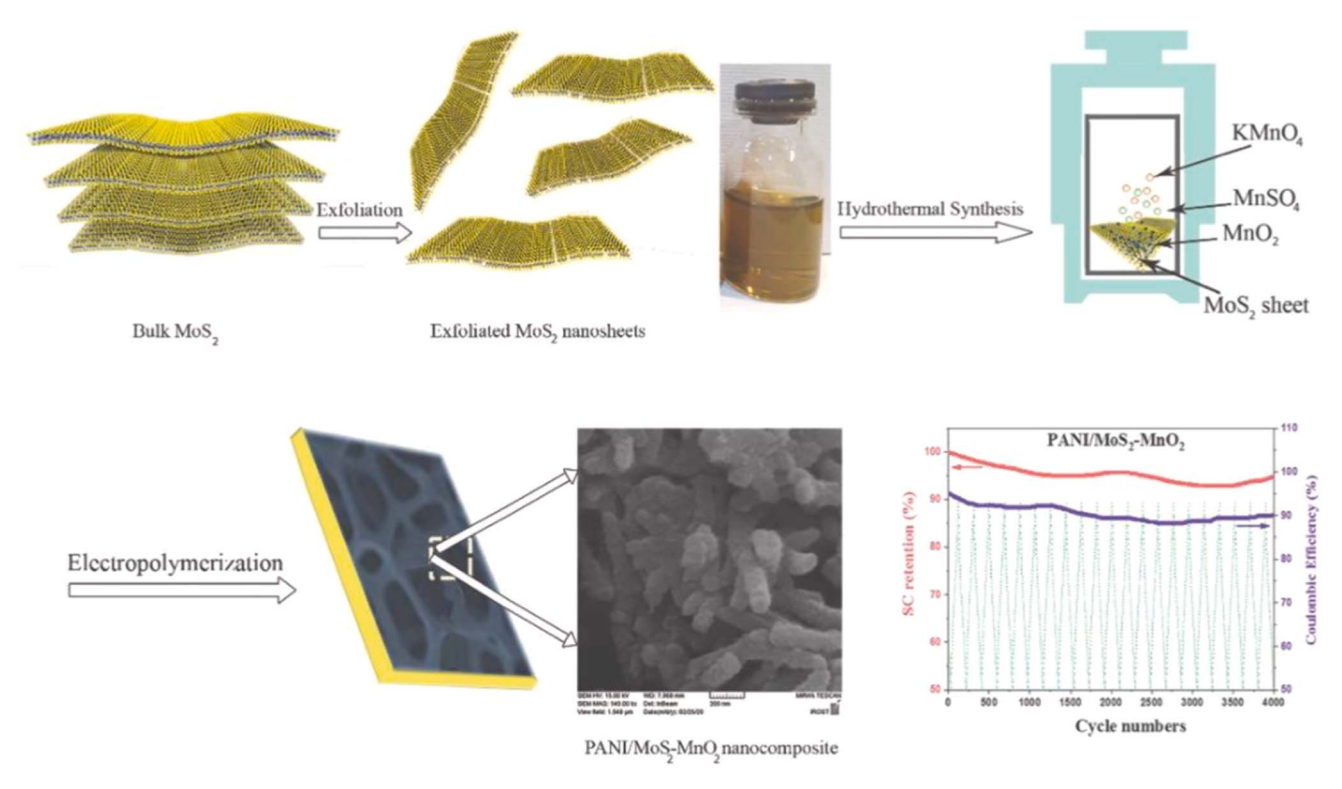


Fig. 11 Synthesis route for ternary PANI/MoS₂-MnO₂ hybrid nanocomposite. 147

3.2 Polypyrrole

Polypyrrole (PPy) is another widely researched π -electron conjugated conducting polymer due to its good electrical conductivity, good environmental stability in ambient conditions, and fewer toxicological problems. Among the various CPs, PPy has been extensively studied because of its ease of processing, stable oxide form, excellent oxidation, and reduction properties, high conductivity, cost-effective and available monomers, as well as good electrical and optical properties. ^{118,149,150} PPy is made up of alternate single and double-bounded macromolecular chain structures and derived its excellent performance from its structure. It is widely considered a potential electroactive material for supercapacitors due to its unique attributes such as higher theoretical capacitance (620 F g⁻¹), improved electrical conductivity, fast charge/discharge capability, and high specific energy. ¹¹⁸

PPy are very adaptable for a variety of applications and have several benefits over other kinds of composites. Because of its intrinsic conductivity, ¹⁵¹ which allows for effective electrical signal transmission, and its high level of biocompatibility, ¹⁵² PPy can be used in biomedical applications such tissue engineering scaffolds and implanted electrodes. It may be created using a variety of techniques, including chemical polymerization and electrochemical deposition, and has cost-effective production route. It is also ecologically stable. Furthermore, by modifying the synthesis conditions and adding dopants, the mechanical and electrical conductivity of PPy may be customized, enabling optimization in applications like as biomedical devices, sensors, and energy storage devices. ^{153,154} The distinct

characteristics of PPy-based nanocomposites set them apart from other composites. They are perfect for situations where weight is a crucial consideration since they are more flexible and lighter than metal-based composites while yet having adequate electrical conductivity. Because PPy is a polymer, it can be processed into complicated forms more easily than ceramic-based composites, providing more design freedom.

However, drawbacks such as poor capacitance and cycling stability have limited its usage in high-performance supercapacitors. Other obstacles to overcome include processing issues when creating intricate structures for particular uses and limited mechanical strength that can call for reinforcement with other materials. PPy nanocomposites continue to be an affordable, highly adaptable material for cutting-edge technology in spite of these difficulties.

Also, as a conjugated conducting polymer, the brittleness of PPy limits its practical uses. The processability and mechanical properties of this material can be improved either by blending PPy with some polymers or by forming copolymers of PPy. It is a fact that biodegradable polymers are preferred to non-biodegradable polymers in recent times, hence, some of the biodegradable polymers that are being used as supercapacitors are; chitosan (CS), PVA, and glycerol. ¹⁴⁹ On the other hand, gum arabic (GA) in the composite form can be used to alleviate the pure PPy problems. The insertion of GA into the PPy matrix can be a promising choice due to its high contact area, chemical, thermal, and mechanical stabilities as well as its high energy storage capabilities at the electrode/electrolyte interface. ¹⁵⁷ Thus, PPy-based composites may provide the fibers or fabrics

This article is licensed under a Creative Commons Attribution-NonCommercial 3.0 Unported Licence. Open Access Article. Published on 10 Machi 2025. Downloaded on 01/11/2025 00:39:34.

Table 3 Electrochemical performance of various supercapacitors fabricated based on polyaniline electroactive material

1045.3 F g ⁻¹ at 1 Ag ⁻¹ 1045.3 F g ⁻¹ at 1 Ag ⁻¹ 1045.3 F g ⁻¹ at 1 Ag ⁻¹ 105.5 F g ⁻¹ at 1 Ag ⁻¹ 105.5 F g ⁻¹ at 1 Ag ⁻¹ 106.5 F g ⁻¹ at 1 Ag ⁻¹ 107.5 F G ⁻¹ at 1 Ag ⁻¹ 1	Conducting polymer	Incorporated materials	Fabrication technique	Structure	Specific capacitance $(F\ g^{-1})$	Capacity retention (cycle numbers)	Power density $(W h kg^{-1})$	Application	References
Carbon dots n star chemical 1 A B 1 at 1 A B 1 Carbon dots n star chemical 676 F g 1 at 1 A B 1 Outdartee polymerization 400 BaMnO, Surfacent-sissisted Nanocrystalline 560.5 F g 1 at 1 A B 1 AAWCNTS Uphancitation Homogenous 248 F g 1 at 1 A B 1 AAWCNTS Utrassories Homogenous 248 F g 1 at 1 A B 1 ZaCO, Q, (B) MGO Thermal reduction Plate simped 720 F g 2 at 1 A B 2 ZaCO, Q, (B) MGO Thermal reduction Plate simped 720 F g 2 at 1 A B 2 PCO, Q, (B) MGO Thermal reduction Plate simped 720 F g 2 at 1 A B 2 PCO, Q, (B) MGO The simpolymerization Procus smooth 142 F g 2 at 1 A B 2 BVQ, (CO, Q) MGO In situ polymerization Hierarchal flower 73 F g 2 at 1 A g 2 RCO/NO In situ polymerization Hierarchal flower 129 F g 2 at 1 A g 2 FCO, PETTO Chemical Long uniform, 158 F g 2 at 1 A g 2 FCO, PETTO Chemical Long uniform, 158 F g 2 at 1 A g 2 FCO/TIO, In situ candit	PANI	ZnS/RGO	Hydrothermal		1045.3 F o ⁻¹ at	160% (1000)	349.7	Electrode materials	126
Carbon dots n star chemical 529 Fg ⁻¹ at 1 Ag ⁻¹ Carbon dots n star chemical 676 Fg ⁻¹ at 1 Ag ⁻¹ BAMIO, oxidative n star chemical oxidative Sto.5 Fg ⁻¹ at 1 Ag ⁻¹ 400 BAMIO, polymerization Homogenous 248 Fg ⁻¹ at 1 Ag ⁻¹ 560.5 Fg ⁻¹ at 1 Ag ⁻¹ 400 AAWCNTS Untrasonic Homogenous 248 Fg ⁻¹ at 1 Ag ⁻¹ 56.4% (10 000) 400 AMWCNTS Chemical activation Homogenous 248 Fg ⁻¹ at 1 Ag ⁻¹ 96.4% (10 000) 33.8 Mn ₃ O ₄ Chemical activation Procus staped 720 Fg ⁻¹ at 1 Ag ⁻¹ 96.4% (10 000) 33.8 RCO-O ₂ O ₃ (3) KGO Thermal reduction Procus nanored 90 Fg ⁻¹ at 1 Ag ⁻¹ 90.4.5% (5000) 403 RCO-O ₂ O ₃ (3) KGO In situ polymerization Hicarchal flower 70 Fg ⁻¹ at 1 Ag ⁻¹ 90.5% (5000) 433 RGO/ZnO In situ polymerization Hicarchal flower 225 Fg ⁻¹ at 1 Ag ⁻¹ 90.5% (1000) 77.39 PL/GO Chemical Propherization In situ condidate Procuss finiting rod 525 Fg ⁻¹ at 1 Ag ⁻¹	!		reduction		0				Ì
Carbon dots contained of the state of polymerization or structure free hemical conditions. 676 F g ⁻¹ at 1 A g ⁻¹ or 32% (300) 400 BaMhO, Surfacent-assisted chemical conditions. Surfacent-assisted chemical conditions. Nanocrystalline of 560.5 F g ⁻¹ at 1 A g ⁻¹ or 40% (10 000) 400 AAWCNIN Ultrasonic polymerization polymerization principal control (Co.Q.Q.) Homogenous polymerization principal control (Co.Q.Q.) 248 F g ⁻¹ at 1 A g ⁻¹ or 40% (10 000) 33.8 RCO.Q.Q. (30 NGC) Chemical activation principal control (Co.Q.Q.) Procuos manored polymerization principal control (Co.Q.Q.) 44.5% (300) 33.8 RCO.Z.Q.Q. (30 NGC) In situ polymerization polymerization polymerization in a situ polymerization polymerization polymerization represented flower polymerization polymerization polymerization propried in the state of	PANI	Carbon dots	In situ chemical		$529 \mathrm{F}\mathrm{g}^{-1}\mathrm{at}1\mathrm{A}\mathrm{g}^{-1}$				127
Carbon dots In situ chemical 676 F g" at 1 A g" at 1 A g" at 1 A g" dots by g" at 1 A g"			oxidative polymerization						
BaMnO ₁ Dolymerization Purificative content	РРу	Carbon dots	In situ chemical oxidative		$676 \; \mathrm{F g}^{-1} \; \mathrm{at} \; 1 \; \mathrm{A g}^{-1}$				127
AMWCNTs polymerization polymerization Homogenous particulate (ree polymerization) 248 F g ⁻¹ at 1 A g ⁻¹ pc. 4% (10 000) ZnCO ₂ O ₃ @N-GO Thermal reduction plate shaped particulate shaped 720 F g ⁻¹ at 1 A g ⁻¹ pc. 4% (10 000) 33.8 Mn ₃ O ₄ Chemical activation particulate shaped procus anorod polymerization Procus nanorod polymerization 940 F g ⁻¹ at 1 A g ⁻¹ pc. 67.000) 33.8 GONN[OH] ₂ One-step in situ polymerization Procus nanorod polymerization 143 F g ⁻¹ at 1 A g ⁻¹ pc. 67.000) 40.3 RGO/ZnO In situ polymerization Hierarchal flower-polymerization 40 F g ⁻¹ at 1 A g ⁻¹ pc. 67.000) 40.3 RGO/ZnO In situ polymerization Fiber-like 22.2 F g ⁻¹ at 1 A g ⁻¹ pc. 67.000) 40.3 PL/GO Oxidative polymerization Fiber-like 22.8 F g ⁻¹ at 1 A g ⁻¹ pc. 70.000 73.8 FTO Orbymerization Fiber-like 35.5 F g ⁻¹ at 1 A g ⁻¹ pc. 70.000 73.8 FTO Orbymerization Interconnected fiber pc. 70.000 72.9 F g ⁻¹ at 1 A g ⁻¹ pc. 70.000 77.79 FTO Orbymerization Procuss fibrillar pc. 70.000 72.8 F g ⁻¹ at 1 A g ⁻¹ pc. 70.000 77.79	ANI	$BaMnO_3$	polymerization Surfactant-assisted	Nanocrystalline	$560.5 \mathrm{F g^{-1}} \mathrm{at} 1 \mathrm{A} \mathrm{g^{-1}}$	95% (500)	400		128
Promoting and polymerization Place shellower Porous nanorod 940 Fg^1 at 1.4 g^1 94.5% (3000) 33.8	EN YO	A MAXXONITION	chemical polymerization	Потоководи	040 E m ⁻¹ of 1 A A -1				07
ZnCO_04@N-GO Thermal reduction Phate shaped patriculate 720 F g ⁻¹ at 1 A g ⁻¹ 96.4% (1000) 33.8 Mn,04 Chemical activation Particulate procus 325 F g ⁻¹ at 1 A g ⁻¹ 96.4% (1000) 33.8 FeCo_04 In situ polymerization Procus nanorod 940 F g ⁻¹ at 1 A g ⁻¹ 94.5% (5000) 33.8 GO/Ni(OH)2 One-step in situ Short cluster shape 743 F g ⁻¹ at 1 A g ⁻¹ 95.4% (5000) 403 GO/Ni(OH)2 One-step in situ Procus nanorod 940 F g ⁻¹ at 1 A g ⁻¹ 95.4% (5000) 403 GO/Ni(OH)2 In situ polymerization Hike nanostructure 40 F g ⁻¹ at 1 A g ⁻¹ 95.4% (5000) 403 GO Electro polymerization Fiber-like 223 F g ⁻¹ at 1 A g ⁻¹ 3700 3700 PHL/GO Dolymerization Fiber-like 235 F g ⁻¹ at 1 A g ⁻¹ 90% (1000) 7.79 FTO Chemical Long, uniform, a rough and porous 355 F g ⁻¹ at 1 A g ⁻¹ 90% (1000) 9.09 FGO/TIO2 In situ emulsion Procues finalitat 692 87 F g ⁻¹ at 1 A g ⁻¹ 92.3% (1000) <td>INIW</td> <td>AMMONTS</td> <td>polymerization</td> <td>structure (tree</td> <td>240 F g at 1 A g</td> <td></td> <td></td> <td></td> <td>140</td>	INIW	AMMONTS	polymerization	structure (tree	240 F g at 1 A g				140
Mn ₃ O ₄ Chemical activation parteculate parteculate 33.8 FeCO ₂ O ₄ In situ polymerization Structure 940 F g ⁻¹ at 0.5 A g ⁻¹ 94.5% (5000) 33.8 GO/NI(OH) ₂ One-step in situ Short cluster shape 743 F g ⁻¹ at 1 A g ⁻¹ 94.5% (5000) 403 GO/NI(OH) ₂ In situ polymerization Hierarchal flower 701 F g ⁻¹ at 1 A g ⁻¹ 95.4% (5000) 403 GO Electro polymerization Hierarchal flower 704 F g ⁻¹ at 1 A g ⁻¹ 85% (5000) 403 GO Electro polymerization Fiber-like 223 F g ⁻¹ at 1 A g ⁻¹ 85% (5000) 403 PL/GO Oxidative Fiber-like 225 F g ⁻¹ at 1 A g ⁻¹ 90% (1000) 73.8 FTO Chemical Long, uniform, 550 F g ⁻¹ at 1 A g ⁻¹ 90% (1000) 7.79 FTO Chemical Long, uniform, 550 F g ⁻¹ at 1 A g ⁻¹ 90% (1000) 7.79 FTO Chemical Long, uniform, 602.87 F g ⁻¹ at 1 A g ⁻¹ 92.3% (1000) 9.09 FTO Chemical In s	ANI	$\mathrm{ZnCO_2O_4}(3)\mathrm{N-GO}$	Thermal reduction	branches) Plate shaped	$720 \; \mathrm{F} \; \mathrm{g}^{-1} \; \mathrm{at} \; 1 \; \mathrm{A} \; \mathrm{g}^{-1}$	96.4% (10000)		Catalytic materials for	130
Structure Peco ₂ O ₄ In situ polymerization Porous nanored 940 F g ⁻¹ at 1 A g ⁻¹ 94.5% (5000)	ANI	$\mathrm{Mn_3O_4}$	Chemical activation	particulate Interconnect porous	$325 \mathrm{Fg^{-1}}$ at $0.5 \mathrm{Ag^{-1}}$	90% (10 000)	33.8	supercapacitors Electrochemical energy	131
GO/Ni(OH)2 One-step in situ Short cluster shape 743 Fg ⁻¹ at 1 Ag ⁻¹ Polymerization Hierarchal flower- 701 Fg ⁻¹ at 1 Ag ⁻¹ 95.4% (5000) 403 RGO/ZnO	ANI	${ m FeCo_2O_4}$	In situ polymerization	structure Porous nanorod	940 F $\rm g^{-1}$ at 1 A $\rm g^{-1}$	94.5% (5000)		storage Advanced energy	132
BiVO4 Dolymerization Hierarchal flower 701 F g^{-1} at 1 A g^{-1} 95.4% (5000) 403 RGO/ZnO	ANI	$GO/Ni(OH)_2$	One-step in situ	Short cluster shape	$743 \; \mathrm{F} \; \mathrm{g}^{-1} \; \mathrm{at} \; 1 \; \mathrm{A} \; \mathrm{g}^{-1}$			storage devices Electrode materials for	133
RGO/ZnO In situ polymerization 40 F g ⁻¹ at 0.05 A g ⁻¹ 86% (5000) 403 GO Electro polymerization 429 F g ⁻¹ at 1 A g ⁻¹ P g ⁻¹ at 10 A g ⁻¹ P g ⁻¹ at 10 A g ⁻¹ 3700 PIL/GO Oxidative polymerization FFD 10 H ₂ SO ₄ 10 H ₂ SO ₄ TiO ₂ /FTO Chemical caction Long, uniform, a rough and portors 550 F g ⁻¹ at 1 A g ⁻¹ P g ⁻¹ p 0% (1000) 73.8 FTO Chemical interconnected fiber structure with a rough and portors structure with a rough and portors 10 S F g ⁻¹ at 1 A g ⁻¹ P g ⁻¹ at 0 M g ⁻¹ P g ⁻¹ at 0 M g ⁻¹ P g ⁻¹ at 1 A g ⁻¹ P g ⁻¹ B g ⁻¹	ANI	BiVO_4	polymerization <i>In situ</i> polymerization	Hierarchal flower- like nanostructure	701 F g^{-1} at 1 A g^{-1}	95.4% (5000)		supercapacitors Electrochemical energy storage	134
GO Electro polymerization Fiber-like 2.23 Fg ⁻¹ at 1 A g ⁻¹ PIL/GO Oxidative Piber-like 2.23 Fg ⁻¹ at 10 Ag ⁻¹ Polymerization Fiber-like 2.25 Fg ⁻¹ at 10 Ag ⁻¹ FTO Chemical Long, uniform, 550 Fg ⁻¹ at 1 A g ⁻¹ FTO Chemical Interconnected fiber 355 Fg ⁻¹ at 40 Ag ⁻¹ FTO Polymerization Porous fibrillar, rod- 692.87 Fg ⁻¹ at 1 Ag ⁻¹ FTO Polymerization Porous fibrillar, rod- 692.87 Fg ⁻¹ at 1 Ag ⁻¹ FTO Polymerization Porous fibrillar, rod- 692.87 Fg ⁻¹ at 1 Ag ⁻¹ FTO Polymerization Porous fibrillar, rod- 692.87 Fg ⁻¹ at 1 Ag ⁻¹ FTO Polymerization Porous fibrillar, rod- 694 Fg ⁻¹ at 1 Ag ⁻¹ FTO Polymerization Porous fibrillar, rod- 694 Fg ⁻¹ at 1 Ag ⁻¹ FTO Polymerization Porous fibrillar, rod- 694 Fg ⁻¹ at 1 Ag ⁻¹ FTO Polymerization Porous fibrillar, rod- 694 Fg ⁻¹ at 1 Ag ⁻¹ FTO Polymerization Porous fibrillar, rod- 694 Fg ⁻¹ at 1 Ag ⁻¹ FTO Polymerization Porous fibrillar, rod- 694 Fg ⁻¹ at 1 Ag ⁻¹ FTO Polymerization Porous fibrillar, rod- 694 Fg ⁻¹ at 1 Ag ⁻¹ FTO Polymerization Porous fibrillar, rod- 694 Fg ⁻¹ at 1 Ag ⁻¹ FTO Polymerization Porous fibrillar, rod- 694 Fg ⁻¹ at 1 Ag ⁻¹ FTO Polymerization Polymerizatio	ANI	RGO/ZnO	In situ polymerization		$40 \mathrm{Fg^{-1}}\mathrm{at}0.05\mathrm{Ag^{-1}}$	86% (5000)	403	Energy storage device	135
FTO Chemical Long, uniform, 550 Fg ⁻¹ at 1A Ag ⁻¹ FTO Chemical Long, uniform, 550 Fg ⁻¹ at 40 Ag ⁻¹ FTO Chemical Long, uniform, 550 Fg ⁻¹ at 40 Ag ⁻¹ FTO Chemical Long, uniform, 550 Fg ⁻¹ at 40 Ag ⁻¹ Structure with a rough and porous morphology FGO/TiO ₂ In situ emulsion Porous fibrillar, rod- 692.87 Fg ⁻¹ at 1 Ag ⁻¹ PTP/TiO ₂ In situ oxidative Entangled thread- 256 Fg ⁻¹ at 1 Ag ⁻¹ FTO Chemical Cookie structure Cookie Co	ANI	GO, IId	Electro polymerization	Tibon 1312	429 F g^{-1} at 1 A g^{-1}		2100	Supercapacitors	136
FTO Chemical Long, uniform, 550 F g ⁻¹ at 1 A g ⁻¹ , 90% (1000) 73.8 FTO Chemical Interconnected fiber 355 F g ⁻¹ at 40 A g ⁻¹ Structure with a rough and porous morphology rGO/TiO ₂ In situ emulsion Porous fibrillar, rod- 692.87 F g ⁻¹ at 1 A g ⁻¹ PTP/TiO ₂ In situ oxidative Entangled thread- 256 F g ⁻¹ at 1 A g ⁻¹ POlymerization Ike network G54 F g ⁻¹ at 1 A g ⁻¹ MoS ₂ In situ oxidative Urchin structure 654 F g ⁻¹ at 1 A g ⁻¹ POlymerization rGO/PET Hydrothermal-assisted Porous 99 F g ⁻¹ at 1 A g ⁻¹ POlymerization sheet like structure 18 89.3% (1000) 46.2	AINI	FIL/ GO	polymerization	ribei-like	$225 \mathrm{Fg}$ at 10 Ag in $\mathrm{H}_2\mathrm{SO}_4$		3700	,	148
FTO Chemical Long, uniform, 550 F g ⁻¹ at 1 A g ⁻¹ , 90% (1000) 73.8	ANI	${ m TiO_2/FTO}$	Hydrothermal reaction		78 F g ⁻¹ at of 1 A g ⁻¹			Electrode for supercapacitors	138
rGO/TiO ₂ In situ emulsion Porous fibrillar, rod- 692.87 F g ⁻¹ at 85.5% (1000) 7.79 polymerization like, and break 0.02 A g ⁻¹ PTP/TiO ₂ In situ oxidative Entangled thread- 256 F g ⁻¹ at 1 A g ⁻¹ 92.3% (3000) 9.09 polymerization like network 654 F g ⁻¹ at 1 A g ⁻¹ 89% (2000) polymerization rGO/PET Hydrothermal-assisted Porous 99 F g ⁻¹ at 1 A g ⁻¹ 98.3% (1000) 46.2 chemical sheet like structure	ANI	FTO	Chemical polymerization	Long, uniform, interconnected fiber structure with a rough and porous	550 F g ⁻¹ at 1 A g ⁻¹ , 355 F g ⁻¹ at 40 A g ⁻¹ ,	90% (1000)	73.8	Current collector in symmetric supercapacitors	117
PTP/TiO ₂ In situ oxidative Entangled thread- 256 F g ⁻¹ at 1 A g ⁻¹ 92.3% (3000) 9.09 polymerization like network MoS ₂ In situ oxidative Urchin structure 654 F g ⁻¹ at 1 A g ⁻¹ 89% (2000) polymerization rGO/PET Hydrothermal-assisted Porous 99 F g ⁻¹ at 1 A g ⁻¹ 98.3% (1000) 46.2 chemical interconnected sheet like structure	ANI	${ m rGO/TiO}_2$	<i>In situ</i> emulsion polymerization	Porous fibrillar, rod- like, and break cookie structure		85.5% (1000)	7.79	Cost-effective and ecofriendly energy storage device	139
MoS ₂ Institutoriation rGO/PET Hydrothermal-assisted Porous Polymerization rGO/PET Hydrothermal assisted Porous Polymerization Sheet like structure	ANI	$\rm PTP/TiO_2$	In situ oxidative	Entangled thread- like network	$256 \text{ F g}^{-1} \text{ at 1 A g}^{-1}$	92.3% (3000)	60.6	Electrode materials for	140
rGO/PET Hydrothermal-assisted Porous $99 \mathrm{Fg}^{-1} \mathrm{at} 1 \mathrm{Ag}^{-1}$ $98.3\% (1000)$ 46.2 chemical interconnected polymerization sheet like structure	ANI	MoS_2	In situ oxidative	Urchin structure	$654 \; \mathrm{F} \; \mathrm{g}^{-1} \; \mathrm{at} \; 1 \; \mathrm{A} \; \mathrm{g}^{-1}$	89% (2000)		Hybrid supercapacitors	141
	ANI	rGO/PET	Hydrothermal-assisted chemical polymerization	Porous interconnected sheet like structure	99 F g^{-1} at 1 A g^{-1}	98.3% (1000)	46.2	High-tech supercapacitors in future electronics	143

Table 3 (Contd.)

Conducting polymer	Incorporated materials	Fabrication technique	Structure	Specific Capacity retentic capacitance (F g^{-1}) (cycle numbers)	Capacity retention (cycle numbers)	Power density $(W h kg^{-1})$	Application	References
PANI	$CS/GM/ Fe_3O_4$	In situ chemical		1513.4 F g^{-1} at	%8'66		Supercapacitors	143
PANI	Co_3O_4	Hydrothermal and <i>in</i>	Irregular layered	4 A 6 3 $^{105.46}$ F $^{g^{-1}}$ at	74.81% (3000)	58.84	High-performance	144
PANI	G-MS	Spray-drying and chemical reduction	Micro-spherical	$596.2 \text{ Fg}^{-1} \text{ at}$ $0.5 \text{ Ag}^{-1},447.5 \text{ F}$	83.70 (1500)		Electrode materials for supercapacitors	133
PANI	CNO	In situ oxidative	Mesoporous	g^{-1} at 20 A g^{-1} 196 F g^{-1} at 1 A g^{-1}	94%		Supercapacitors	145
PANI	rGO/B	polymenzation Photolithography, colloidal lithography, and soft-template		$614 \mathrm{Fg}^{-1} \mathrm{at} 1.0 \mathrm{Ag}^{-1}$	85% (10 000)		Electrochemical energy storage in flexible devices	146
PANI	MoS ₂ -MnO ₂	techniques Hydrothermal and electro-polymerization	Larger porous structure	$479~{ m F~g}^{-1}$	94.1% (4000)	35.97	Electro-active material for energy storage devices	147

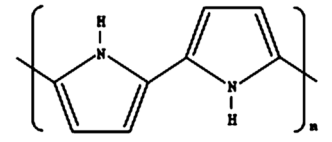


Fig. 12 Molecular structure of polypyrrole. 158

with electrical properties similar to metals or semiconductors. Fig. 12 reveals how PPy is prepared by an oxidative polymerization process. It can be made either chemically through solution processing or electrochemically through polymer deposition at an electrode and both processes involve electron transfer. The polymerization proceeds *via* the radical cation of the monomer that reacts with a second radical cation to give a dimer by the elimination of two protons. Dimers and higher oligomers are also oxidized and react further with the radical cations to build up the PPy chain.

Polypyrrole is an example of a heterocyclic conductive polymer. Electrochemical synthesis of polypyrrole in sulfuric acid yielded a black conducting film that is stable under ambient conditions and even at temperatures above 200 °C. The electrical and mechanical properties of the electropolymerized polypyrrole film depend heavily on the counter-ion used. Using perchlorate instead of oxalate can increase its conductivity by 10 times. Commercially available polypyrrole films with tosylate counter-ions are highly conductive (15 S cm⁻¹) and are very stable under ambient conditions (conductivity only decreased by 15% after 1 year). To increase the processability of polypyrrole, soluble forms were synthesized by adding flexible side chains along the ring. The addition of various functionalities at the nitrogen can also improve its solubility; however, the conductivity of the resulting film can be reduced drastically because of the strong steric interactions of the substituent at the nitrogen and the hydrogens at the 3- and 4-positions of the adjacent pyrrole rings. The adjacent rings are forced out of the plane which results in loss of conjugation and ultimately drastic reduction of its conductivity. Although polypyrrole is the most intensively studied representative of π -conjugated conducting polymers, many important questions on how to create its properties for a variety of specific applications remain open or await improvement. A theoretical study on the competition between polarons and bipolarons in nondegenerate conjugated polymers revealed that charge carriers at low doping concentrations are most likely polarons. The model predicted the transition from a polaron lattice to a bipolaron lattice with an increasing doping level. The calculations were consistent with former ESR results on polypyrrole doped with monoanionic. Ion transport in polypyrrole electrodes undergoing a reversibleredox process mostly focused on single-charged counterions.

The structure and reactivity of conducting polymers are influenced by multi-charged redox inert counterions. Despite the large collection of data concerning the effects of electrolyte anions and cations on the electrodeposition and performance of polypyrrole electrodes, the data for multicharged inorganic counterions were scarce and dominated by sulfates. It was suggested that sulfates, which were called "unfavorable" ions,

Review **RSC Advances**

may strongly associate with the positive sites of polypyrrole chains which can result in electrostatic cross-linking, thus, leading to a compact film structure and the low mobility of charge carriers.

PPy is readily polymerized in an aqueous solution by a wide variety of oxidizing agents like FeCl₃, (NH₄)₂S₂O₈, and CuCl₂. The reaction speed is higher in the case of (NH₄)₂S₂O₈ (a few minutes) and is slower for FeCl₃ (e.g. 6 hours) with different kinds of dopants being used. Dopant concentration has the same effect on the reaction speed as oxidants; an increase in dopant concentration slows down the polymerization reaction. It has been demonstrated that additives like anion surfactants can increase the conductivity of chemically synthesized PPy. The addition of sodium bis(2-ethyl)sulfosuccinate (AOT) into the polymerization solution including Fe₂(SO₄)₃ as an oxidant improved the conductivity of PPy by several orders of magnitude depending on the PPy/AOT ratio. The chemical oxidative polymerization method for PPy synthesis is recommended if a large amount of polymer is needed. By applying this method PPy can be deposited both onto conducting and non-conducting substrates like metals, glass, plastic, textile, etc. In the case of an electrochemical preparation typically PPy films are galvanically deposited on a platinum electrode surface using a onecompartment cell containing an aqueous solution of pyrrole and oxidizing agent.

Ullah et al. 157 synthesized PPy by using a pyrrole monomer via inverse emulsion polymerization as shown in Fig. 13. The procedure was carried out in a three-necked round bottom flask holding 35 mL toluene and 10 mL 2-propanol that was stirred for 15 min. After that, 200 μL of pyrrole was added and stirred for another 15 min, followed by the dropwise addition of 0.5 mL of DBSA and 0.303 g of benzoyl peroxide (dissolved in 5 mL of water) to the reaction mixture. To get the precipitate, the mixture was vigorously stirred for 24 h. The precipitate was washed three times with distilled water and 50 mL of acetone to separate the pure product that was dried in an oven at 50 °C for 24 h.

Another method of preparing pyrrole and also thiophene polymers is plasma polymerization. The usual procedure, in this case, is that the monomer is first plasma polymerized in the form of a thin film on top of the substrate. Then the specimens are exposed to the vapors of the doping agent (e.g. iodine) to introduce charge carriers into the plasma-polymerized structures. The resulting polymer structures have proven to have higher degree of cross-linking and branching. The morphology of those films is smoother and more uniform than chemically polymerized analogs but electrical conductivity (in the order of $10^7 - 10^9 \,\Omega^{-1} \,\mathrm{mm}^{-1}$) and environmental stability are poor. Although PPy is prepared in its oxidized conducting state, the resulting polymer can be subsequently reduced to give the insulating form. Reversible electrochemical switching between the conducting and insulated state causes a color change from blue-black to vellow-green.

Designs of PPy electroactuators encompass a monolithic, bilayered, or trilayered structure. Monolithic and bilayered implementations are primarily used in applications involving a supporting liquid electrolyte (either aqueous or organic) while trilayered ones are employed with an ionic gel electrolyte sandwiched between two PPy films for operation in air. Due to longitudinal voltage attenuation along a semiconducting CP strip, a monolithic electroactuator tail usually generates a smaller strain than its upper section resulting in a notable strain gradient along the strip.159

Barazandeh and Kazemi, 160 introduce a simple and facile process to prepare a dandelion-like NiCo2S4/PPy nanomaterial

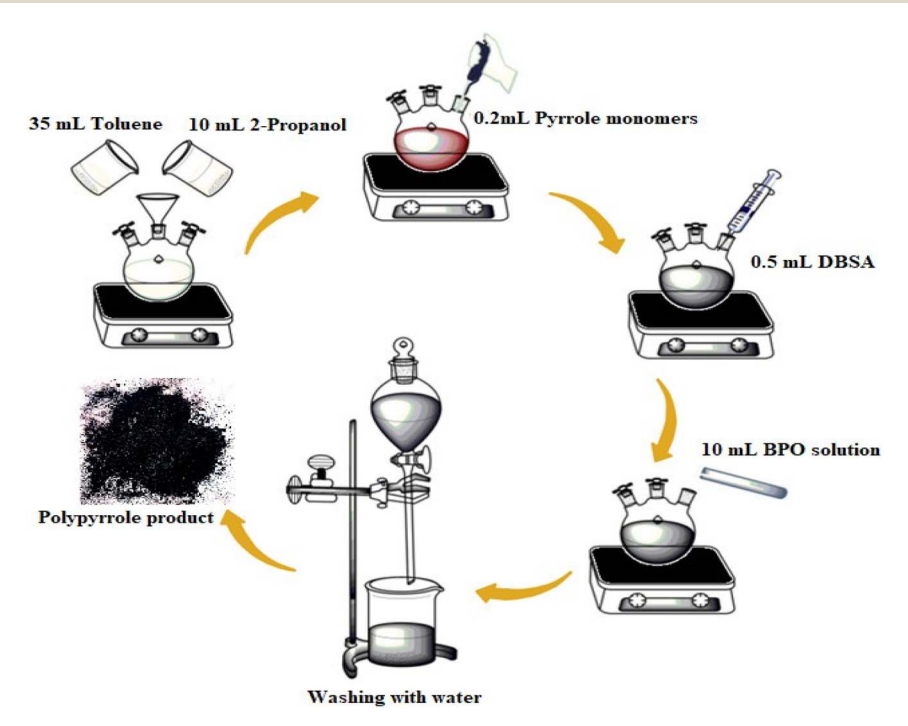


Fig. 13 Synthesis route for polypyrrole. 157

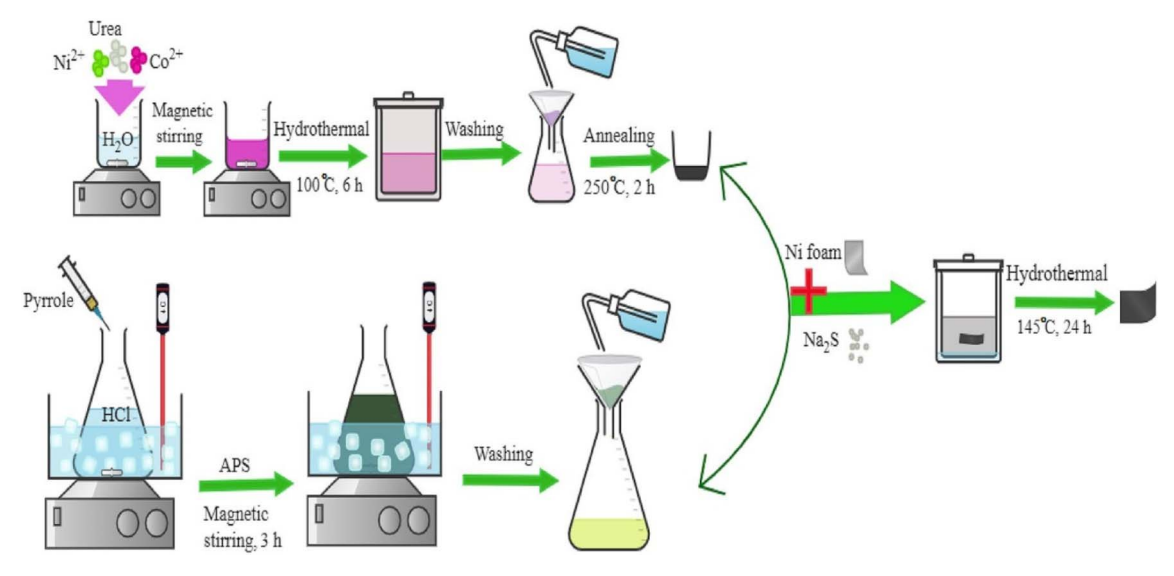


Fig. 14 Schematic representation of NiCo₂S₄@PPy nanomaterial fabrication. ¹⁶⁰

for supercapacitor application. In the method, NiCo₂S₄@PPy was directly deposited on a nickel foam substrate. The combination of NiCo₂S₄ and polypyrrole, and direct deposition of this material on nickel foam (NF) resulted in excellent capacitive performance such as high capacitance, good cycle life stability, and significant conductivity. Moreover, an asymmetric device based on NiCo2S4@PPy/NF and rGO/NF electrodes was assembled. It exhibited a specific capacitance of almost 98.9 F g⁻¹ with an energy density of 35.17 W h kg⁻¹ at a power density of 1472 W kg⁻¹. These results indicate that NiCo₂S₄@PPy/NF is a promising electrode for supercapacitor application. The fabrication steps of a NiCo2S4@PPy composite electrode are shown in Fig. 14. In the first step, NiCo₂S₄ was prepared via the hydrothermal process which ended with a calcination treatment. Simultaneously, polypyrrole (PPy) was prepared by the chemical oxidative polymerization method. Then, the NiCo₂-S₄@PPy nanomaterial was deposited on the Ni foam substrate through a facile hydrothermal method.

In the study carried out by Bashid *et al.*,⁵⁸ nanocomposite comprising polypyrrole and reduced graphene oxide was electrodeposited onto a carbon bundle fiber (CBF) through a two-

step approach (CBF/PPy-rGO-2) as shown in (Fig. 15). The CBF/PPy-rGO-2 had a highly porous structure compared to a nanocomposite of polypyrrole and reduced graphene oxide that was electrodeposited onto a CBF in a one-step approach (CBF/PPy-rGO), as observed through a field emission scanning electron microscope. An X-ray photoelectron spectroscopic analysis revealed the presence of a hydrogen bond between the oxide functional groups of rGO and the amine groups of PPy in the PPy-rGO-2 nanocomposite. The fabricated CBF/PPy-rGO-2 nanocomposite material was used as electrode material in a symmetrical solid-state supercapacitor, and the device yielded a specific capacitance, energy density, and power density of 96.16 F g^{-1} , 13.35 W h kg^{-1} and of 322.85 W kg^{-1} , respectively. Moreover, the CBF/PPy-rGO-2 showed capacitance retention of 71% after 500 consecutive charge/discharge cycles at a current density of 1 A g⁻¹. The existence of a high degree of porosity in CBF/PPy-rGO-2 significantly improved the conductivity and facilitated ionic penetration. The CBF/PPy-rGO-2-based symmetrical solid-state supercapacitor device demonstrated outstanding pliability because the cyclic voltammetric curves remained the same upon bending at various angles.

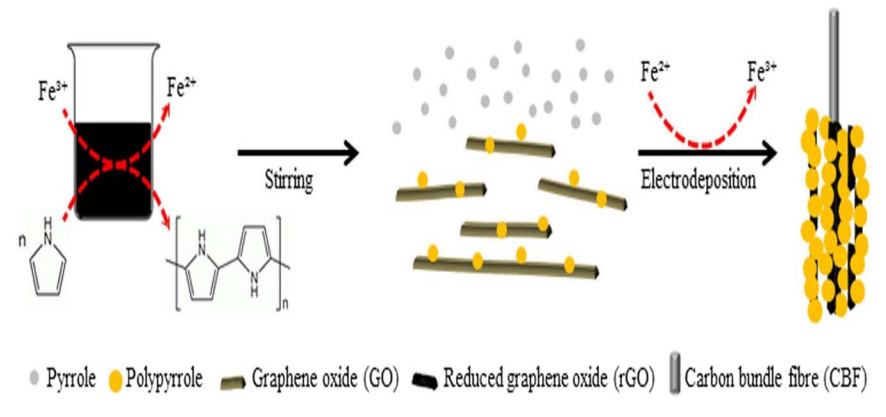


Fig. 15 Schematic diagram of the synthesis process of CBF/PPy-rGO-2.58

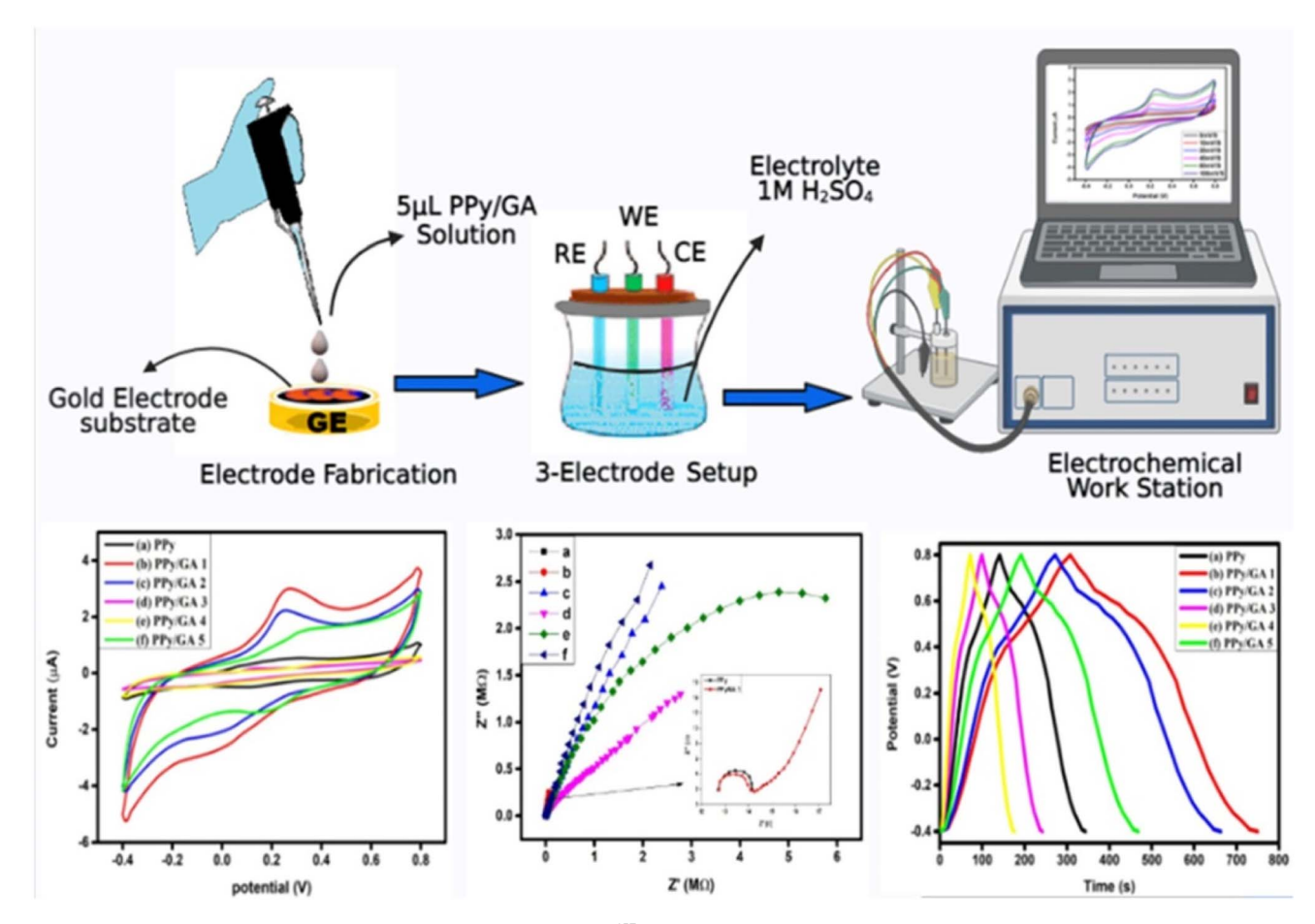


Fig. 16 Electrode fabrication towards electrochemical properties. 157

In this research that was carried out by Ullah et al. 157 an electrode for a supercapacitor based on PPy/GA composites was fabricated by inverse emulsion polymerization as shown in Fig. 16. The electrochemical characteristics, cyclic voltammetry (CV), electrochemical impedance spectroscopy (EIS), and galvanometric charging-discharging (GCD) properties of the fabricated PPy/GA composites-based supercapacitor devices were investigated. The synthesized material shows good electrochemical properties in terms of using cyclic voltammetry, galvanostatic charging-discharging, and EIS tests. PPy has the lowest specific capacitance, energy density, and power density, with values of 168.6 F g⁻¹, 33.698 W h kg⁻¹, and 599.37 W kg⁻¹ respectively. With a 0.125 wt% loading of gum arabic in polypyrrole, these values were enhanced to 368.57 F g⁻¹, 73.667 W h kg⁻¹, and 599.609 W kg $^{-1}$, at a current density of 1 A g $^{-1}$.

3.3 Poly(3,4-ethylene dioxythiophene)

Poly(3,4-ethylene dioxythiophene) commonly referred to as PEDOT is a conjugated polymer that carries positive charges upon doping. PEDOT belongs to the polythiophene family and has emerged as a promising candidate for pseudocapacitor electrodes owing to its fast electrochemical kinetics and excellent intrinsic conductivity.161-163 It can be synthesized chemically or electrochemically. It is typically used as a transparent and conducive polymer with high ductility in various applications. It has wide applications in energy conversion and storage devices. PEDOT is a chemically stable, conjugated polymer that is of considerable interest for a variety of applications in organic solar cells, dye-sensitized solar cells, supercapacitors, fuel cells, thermoelectric devices, and stretchable devices. Among conducting polymers, PEDOT is significantly important due to its small band gap, high conductivity, and high stability.164 PEDOT has a small band gap structure as shown in Fig. 17 that allows it to be utilized in several applications such as organic light-

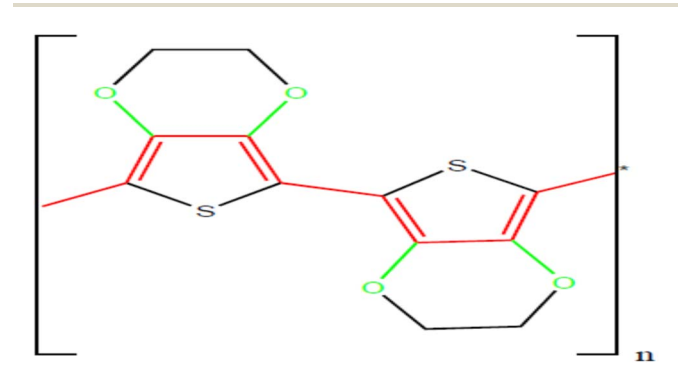


Fig. 17 Chemical structure of conjugated conductive polymer poly(3,4-ethylene dioxythiophene).163

emitting diodes, photovoltaics electroluminescent devices, antistatic coatings, and capacitors. 163,165

The overall performance of chemosensors is determined by several factors such as sensing material's chemical and physical properties, device geometry, and signal transduction. Improvement of the sensor performance demands a synergistic optimisation of the abovementioned factors. In terms of sensing materials, diverse conductive materials such as conducting polymers, polymer/carbon composites, graphene, and metal or semiconductor nanocrystals show great promise. Especially, conducting polymers such poly(3,4ethylenedioxythiophene) (PEDOT), polypyrrole (PPy), and polyaniline (PANI) are among the highest attractive sensing materials owing to their intriguing features such as their all-organic nature with good designability, intrinsic electrical conductivity, high signal transduction, dimensional durability, mechanical flexibility and chemical stability.166 The syntheses of the polymers, usually via convenient chemical or electrochemical polymerization methods are simple and cost-effective. 167,168 The polymers thus synthesized can retain their electrical conductivity and chemical/physical stability when used in chemosensors. Such durability is crucial for chemosensors, for which sensing repeatability is one of the most important factors affecting the real application of sensor devices. 169

Several elements, including the device's geometry, signal transduction, and the chemical and physical characteristics of the sensing material influence chemosensor performance. The above-mentioned elements must be optimized synergistically to improve sensor performance. Diverse conductive materials, including conducting polymers, polymer/carbon composites, graphene, and metal or semiconductor nanocrystals, hold considerable potential as sensing materials. Conducting polymers in particular, like poly(3,4-ethylenedioxythiophene) (PEDOT), polypyrrole (PPy), and polyaniline (PANI), are among the most alluring sensing materials due to their intriguing characteristics, including their all-organic nature with good designability, intrinsic electrical conductivity, high signal transduction, dimensional durability, mechanical flexibility, and chemical stability. Polymers are usually created cheaply

and easily using convenient chemical or electrochemical polymerization processes. 166,170 Fig. 18 illustrates the methods for preparing aligned PEDOT nanofibres and PEDOT nanotubes by oxidative polymerization of EDOT monomer incorporated in oriented assemblies of electrospun PLGA/PCL nanotubes. 163

However, pristine PEDOT electrodes are unstable upon repetitive cycling, and their capacitance is lower compared to other pseudocapacitive materials. 171 Various strategies have been explored in the past decade, mainly in the synthesis of PEDOT composites with carbon nanomaterials and metal oxides. One interesting approach to take advantage of the characteristics of EDLC-type systems and pseudocapacitors consists of the addition of carbon particles into the polymer matrix of CPs to obtain a composite material. An electrode made of poly(3,4-ethylenedioxythiophene) (PEDOT)-carbon composite exhibited high specific capacitance values and number of cycles due to the semiregular, macroporous nature of the electrode film. 172,173 These advances give way to many other combinations of carbon-conducting polymer composites for energy storage and other applications.

González et al.174 developed a composite material of poly(3,4ethylenedioxythiophene) (PEDOT)/activated carbon (AC) by in situ polymerization and subsequently deposited by spray-coating onto a flexible electrolyte as shown in Fig. 19. Two activated carbons were tested: a commercial activated carbon and a labmade activated carbon from Brewer's spent grain (BSG). The porous and spongy structure of the composite increased the specific surface area, which helps to enhance the energy storage density. This procedure to develop conductive composite materials using AC prepared from biowaste has the potential to be implemented for the preparation of polymer-based conductive inks for further applications as electrodes in pseudocapacitors.

In the last years, alternative carbon materials such as carbon nanotubes or graphene have been proposed as electrode materials for supercapacitors. 175 Very recently, Khasim et al. 176 have developed a high-performance and flexible supercapacitor using a conductive composite material composed of reduced graphene oxide (rGO) and PEDOT-PSS. A doped PEDOT-PSS:ethylene glycol/rGO composite film demonstrated

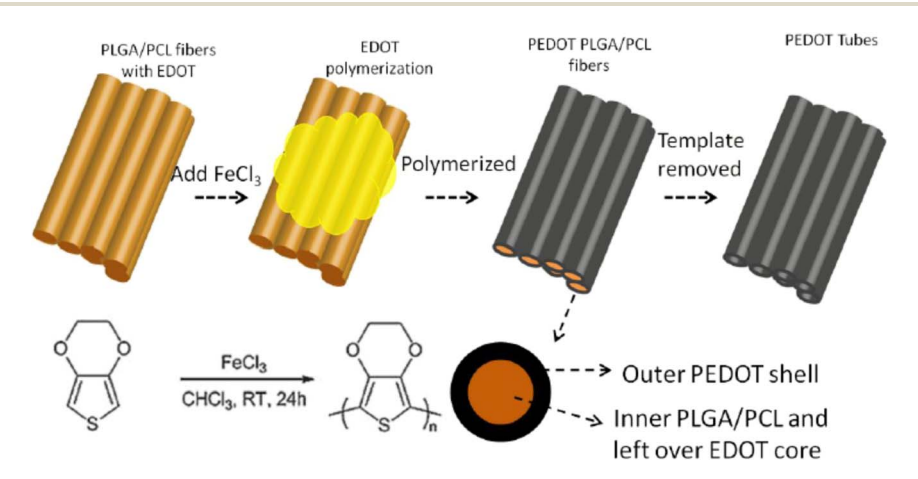


Fig. 18 Schematic illustration of methods for preparing aligned PEDOT nanofibres and PEDOT nanotubes by oxidative polymerization of EDOT monomer incorporated in oriented assemblies of electrospun PLGA/PCL nanotubes. 163

Review RSC Advances

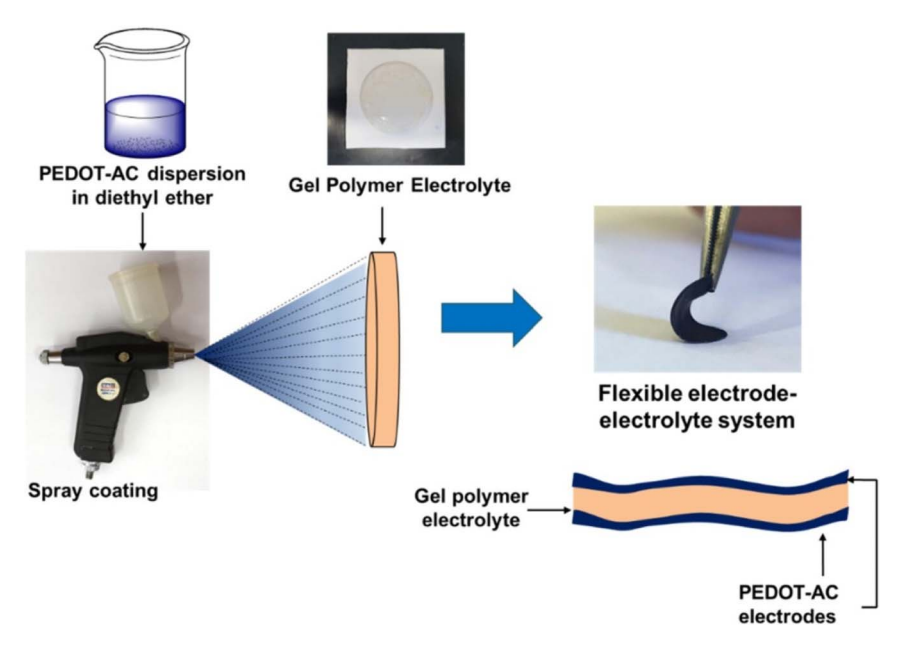


Fig. 19 Preparation of flexible electrode-electrolyte system. 174

Table 4 Conductivity and resistance of different PEDOT/PLGA fibers¹⁶³

Sample	Resistance (k Ω)	Conductivity (mS cm ⁻¹)
8 μm fibers polymerized by 60 wt% FeCl ₃	2.2	2.2
4 μm fibers polymerized by 60 wt% FeCl ₃	4	2.3
2 μm fibers polymerized by 60 wt% FeCl ₃	7.8	2.5
8 μm fibers polymerized by 50 wt% FeCl ₃	13	0.75
$8 \mu m$ fibers polymerized by 30 wt% FeCl ₃	50	0.2

improved electrochemical performances with a specific capacitance of 174 F $\rm g^{-1}$ and energy density of 810 W h $\rm kg^{-1}.$ However, the relatively high price of graphene and the agglomeration of these particles have limited its scalability and application in commercial supercapacitors.

Yang et al. 90 combined structural design and 3D printing techniques to produce additive-free stretchable electrodes with varying negative Poisson's ratio (NPR) structures based on PEDOT:PSS ink. Tensile and finite element analyses (FEA) revealed that the stretchable electrode has a well-designed arc shape NPR structure which can effectively minimize the peak strain and result in excellent flexibility of 180° and maximum stretchability of 150%. Moreover, further incorporation of CNTs into the 3D printed hybrid polymer/CNT electrode enhanced the electrochemical performance of the electrode, exhibiting a high area capacitance of 999 mF cm⁻². These developed quasi-solid state symmetric supercapacitors not only obtain an excellent energy density and satisfactory capacitance retention of 74.7%

after 14 000 cycles but also demonstrated good mechanical properties by maintaining stable power output even when extremely deformed, thus providing a promising step towards the fabrication of stretchable conducting polymer electrodes with excellent mechanical and electrochemical performance for various applications in flexible electronic devices. Table 4 presents the conductivity of different PEDOT/PLGA fibers (8 μ m fibers were spun from a sample with an EDOT/PLGA ratio of 1: 10, 4 μ m fibers were spun from the sample with an EDOT/PLGA ratio of 3: 10, and 2 μ m fibers were spun from the sample with EDOT/PLGA ratio of 5:10) (Jinghang, 2011 ¹⁶³).

Outlook into applications of functional polymers in EDLCs, pseudocapacitors and hybrid capacitors

Polymers have become central to the evolution of supercapacitors, including electric double-layer capacitors (EDLCs), pseudocapacitors, and hybrid designs. Thanks to their adaptable properties such as flexibility, lightweight construction, and customizable conductivity. These functional polymers have significantly enhanced the functionality and versatility of these energy storage devices. By combining polymers with other innovative materials, researchers have achieved breakthroughs in energy and power density, device durability, and creative design possibilities for various applications.^{177,178}

In the realm of EDLCs, energy storage is achieved through electrostatic charge separation at the electrode–electrolyte interface. Polymers play a vital role here by improving the efficiency of this interface. For instance, conducting polymers like polyaniline (PANI), polypyrrole (PPy), and PEDOT (poly(3,4-ethylenedioxythiophene)) are often blended with carbon-based

RSC Advances

progresses, the future of polymer-based supercapacitors looks promising, paving the way for innovative and sustainable energy solutions.

materials such as activated carbon, graphene, and carbon nanotubes (CNTs).¹⁷⁹ These combinations enhance electrical conductivity and structural strength while maximizing the surface area available for energy storage. Additionally, polymeric binders such as polyvinylidene fluoride (PVDF) and Nafion are used to maintain the structural integrity of electrodes during use. The synergy between polymers and nanostructured carbons improves capacitance, reduces internal resistance, and enables the creation of flexible, high-performance devices. As a result, polymer-enhanced EDLCs have found applications in areas like portable electronics, regenerative braking systems, and uninterruptible power supplies, where rapid energy delivery and durability are paramount¹⁸⁰

Pseudocapacitors, which store energy through reversible faradaic reactions on electrode surfaces, also benefit from the unique properties of polymers. These devices rely heavily on conducting polymers like PANI, PPy, and PEDOT due to their ability to support high-speed electron transfer and ion diffusion. PANI is particularly valued for its high capacitance and ease of synthesis, while PPy's flexibility and conductivity make it a versatile choice for various configurations. PEDOT, with its excellent mechanical properties and stability, is another standout material. 181,182 However, challenges such as structural degradation from repeated swelling and shrinking during charge cycles remain. By creating polymer composites that incorporate carbon-based materials or metal oxides, these issues can be mitigated, leading to improved longevity and reliability. 183,184 Pseudocapacitors, with their higher energy densities compared to EDLCs, are particularly suited for applications demanding robust storage capabilities, such as energy grids and advanced portable technologies. 180

Hybrid supercapacitors merge the best features of EDLCs and pseudocapacitors, offering both high power density and increased energy storage. Polymers play a dual role in these systems, both as active materials and as components in hybrid electrodes. Conducting polymers like PANI, PPy, and PEDOT are frequently integrated with materials like manganese dioxide (MnO₂), ruthenium oxide (RuO₂), or graphene to enable simultaneous electrostatic and faradaic charge storage. 185-187 Conducting polymers can be modified with dopants to optimize performance for particular applications, while composite designs enable advanced functionalities like self-repair and thermal regulation. Furthermore, the use of eco-friendly synthesis methods and scalable production techniques ensures that polymer-based supercapacitors are not only highperforming but also environmentally responsible.177,188 Efforts to develop more durable polymer composites continue to address challenges such as cycling stability and conductivity retention, driving the creation of lightweight, long-lasting, and efficient energy storage solutions. The integration of polymers into supercapacitors represents a transformative leap forward in energy storage technology. By combining their inherent properties with cutting-edge material science, polymers have enabled the development of supercapacitors that meet the demands of modern applications, from renewable energy systems to wearable technology and beyond. As research

Applications and impact of polymer nanocomposites

Polymer nanocomposites are increasingly used in flexible packaging due to their ability to enhance barrier properties against gases like oxygen and moisture, improve mechanical strength, and provide functionalities such as UV protection. These characteristics make it possible to develop thinner, more effective packaging materials that prolong shelf life, lower material consumption, and maintain product quality. Nanocomposites enhance durability, and environmental sustainability through the integration of cutting-edge features. 189-195 Polymer nanocomposites play a crucial role in flexible packaging by offering enhanced performance through key applications. The incorporation of nanofillers like clays, silica, or metal oxides significantly improves barrier properties, reducing gas permeability.¹⁹³ Nanoparticles also enhance tensile strength and tear resistance. Additionally, they improve heat-sealing capabilities, ensuring secure closures to minimize contamination risks. UV-absorbing nanoparticles provide added protection by preventing product degradation caused by ultraviolet light exposure.192

Notably, PANI is a widely used material in flexible wearable devices due to its high electrical conductivity, good environmental stability, low cost, and ease of processing into flexible films.196-200 Because of these characteristics, PANI is a great option for wearable electronics that adapt to the human body while still functioning dependably, flexible sensors, 199 and energy storage devices like supercapacitors.200 By altering its conductivity in response to external stimuli, PANI demonstrates excellent sensitivity in flexible sensors, making it possible to detect factors such as pressure, tension, pH, and biomolecules. PANI-based electrodes for electrochemical sensors provide realtime monitoring of body fluids, including perspiration, for medical diagnostic purposes. Furthermore, PANI's high specific capacitance facilitates the creation of wearable electronics supercapacitors, and its incorporation into triboelectric nanogenerators (TENGs) allows devices to be powered by body motion energy collecting.201,202 PANI's mechanical flexibility, which enables it to adapt to curved surfaces without losing functionality, and its adjustable conductivity, which can be doped for certain applications, are two benefits of employing it in wearable technology.203,204 PANI can also become biocompatible with the right surface modification, which qualifies it for skin-contact devices. It is even more appealing for scalable manufacturing because of its low cost.205,206 But issues like doping stability and environmental deterioration need to be addressed. Environmental stability can be enhanced by encapsulation or protective coatings, and sustained conductivity levels over time need meticulous design and production procedures.207 PANI is still a flexible and affordable material for developing wearable technology in spite of these obstacles.

Similarly, PPy offers superior structural stability in contact with body fluids, such as sweat, compared to metals. PPy is valued for its high specific capacitance (480 F g⁻¹), environmental stability, good conductivity, excellent redox properties, and ease of synthesis. It is also biocompatible, minimizing excessive immune responses. While pristine PPy lacks intrinsic antibacterial properties, nanostructured PPy can regulate bacterial viability, such as through PPy nanosuckers that enhance bioelectricity generation in microbial fuel cells. Furthermore, PPy can be tailored into various morphologies, including nanowires, nanospheres, and nanosheets, by modifying polymerization conditions.²⁰⁸

Finally, PEDOT:PSS-based electrochromic devices (ECDs) are gaining prominence in flexible electronics due to their high optical contrast, low energy consumption, bistability, and simple structure. These devices exhibit color changes under voltage, making them ideal for applications like information displays, anti-counterfeiting, and wearable health monitoring. For example, PEDOT:PSS has been used to create recyclable, biodegradable, and eco-friendly ECDs with enhanced optical transmittance, coloration efficiency, and durability, offering significant advantages over conventional materials like PET.^{209,210}

In wearable health monitoring, PEDOT:PSS-based ECDs provide real-time visualization of vital signs, such as glucose or lactate concentrations in sweat, through reversible color changes. These devices are lightweight, compact, and stretchable, enabling efficient, non-invasive health monitoring. Additionally, PEDOT:PSS plays a vital role in flexible energy storage systems, combining energy storage with electrochromic functions for real-time power monitoring and efficient operation. Advances in material design, such as the integration of nanoparticles and conducting polymers, also pave the way for self-powered photovoltaic-electrochromic devices, offering sustainable and maintenance-free solutions for next-generation wearable electronics.^{209,210}

6. Challenges, future demands and expectations

In the modern era, an integral part of human life is smart technology. Accordingly, advanced technologies are always searching for smart and well-fabricated materials to satisfy the growing demand.22,45,79,125 As the progress of the trend, the development of novel materials with improved electrochemical performance is required to address the critical issue of pollution. There is a growing need for sustainable and renewable energy storage solutions in hybrid automobiles and portable electronic devices necessitating the development of innovative materials with better electrochemical capabilities, such as electrochemical capacitors or supercapacitors.211 The application of functional polymers in e-textiles and other related biomedical fields has shown that energy is needed to perform all necessary operations both in living and non-living things for the attainment of human comfort. Hence, the quest for improved, readily available, eco-friendly, and cost-effective sources of energy will be on the increase to avert an energy

Polymer-based materials, nanotechnology, crisis. composite materials development have been the main sources of progress made in the modern days.38 However, the development of functional polymers as supercapacitors still faces several significant challenges that must be overcome to enable their widespread use. One of the primary obstacles is the inefficiency of current production processes, such as photolithography and electroplating. These methods involve multiple phases and strict requirements, which limit their applicability in creating flexible supercapacitors. Simplifying these processes is crucial to improving performance and expanding the use of supercapacitors in various electrical systems. Additionally, the materials used for the electrodes in supercapacitors present limitations. A key challenge lies in developing materials with optimal porosity and increased surface area to enhance energy storage. While materials like metal-organic frameworks (MOFs) and MXenes show promise due to their high surface areas and electrical conductivity, they still require further refinement to fully meet the demands of supercapacitor applications. The lack of systematic methods for designing electrode architectures that effectively address porosity, interlayer spacing, and crystalline structure also restricts the optimization of electrochemical performance.212,213 Improving the electrochemical properties of the polymer materials. Ion doping, including ptype and n-type doping, can enhance the conductivity and performance of electrode materials, but precise doping techniques combined with effective post-heat-treatment processes are necessary to achieve these improvements. Furthermore, other important properties such as thermal stability, machining capacity, and mechanical strength must be considered to ensure that the supercapacitors are not only efficient but also durable and practical for real-world applications. Beyond electrochemical and material concerns, additional features like transparency, self-healing, and photosensitivity need to be explored further to enhance the overall performance of supercapacitors. Incorporating these properties places additional demands on research and development, making the process more complex. Moreover, flexible supercapacitors must be capable of functioning in dynamic environments, such as those subjected to bending. This raises concerns about bending cycle performance and electrolyte leakage, both of which need to be addressed to ensure long-term reliability.

Industrial barriers also impede the large-scale application of supercapacitors with excellent performance. High production costs, technological limitations, and the absence of standardized industry practices make it difficult for high-performance supercapacitors to be manufactured and implemented on a large scale. These barriers must be overcome to enable the broader use of supercapacitors in various industries.

Looking to the future, several research directions hold promise for advancing the field of functional polymers as supercapacitors. One key area of focus is the development of advanced materials with enhanced surface area and conductivity. Continued exploration of materials like MOFs and MXenes could lead to significant improvements in supercapacitor performance. Additionally, as the demand for wearable electronics and smart textiles grows, the development of

fiber-based supercapacitors with foldable, stretchable, and bendable properties will become increasingly important. The integration of these flexible devices with multifunctional capabilities is expected to be a major research trend.

However, there is a need for more technological advancement toward natural resources that will be void of harmful side effects which are the bane of present-day technological developments. Aside from this, many technological limitations of the present times in most developing nations need to be overcome to have a safe global community. This can only be achieved with more intense research and development in electrical and electronic systems-based materials that will aid more transmission of data, resources, information, and many more even from remote areas.

Conclusion 7.

The application of polymers as conductive materials has aided the development of many modern materials and products for human comfort due to their ease of production and modifications. The inherent polymer properties made it the best material among the three fundamental materials for most applications; hence, it is readily available to suit most areas of need. The work considers the effectiveness of polymers as conductive materials and their suitability for the production of supercapacitors for electronic applications. From the review, it was discovered that PANI, PPy, and PEDOT are the most widely used conductive polymers based on their ease of production, all-organic nature with good dimensional durability, mechanical flexibility, and chemical stability in addition to their excellent intrinsic electrical conductivity and high signal transduction. More efforts are to still be focused on polymers through their modifications as this will further provide more easily accessible suitable functional products. This is necessary because the combination of polymer properties and modifications cost is always cost-effective compared to metal and ceramics.

Data availability

No data was used for the research described in the article.

Author contributions

All authors contributed equally to the write-up and revision of this work.

Conflicts of interest

The authors declare that they have no known competing financial interests or personal relationships that could have appeared to influence the work reported in this paper.

References

1 J. L. Espinoza-Acosta, P. I. Torres-Chávez, J. L. Olmedo-Martinez. A. Vega-Rios, S. Flores-Gallardo

- E. A. Zaragoza-Contreras, J. Energy Chem., 2018, 27, 1422-1438.
- 2 M. R. A. Bhuiyan, Micro Nano Lett., 2022, 17, 402-416.
- 3 A. Androniceanu and O. M. Sabie, Energies, 2022, 15, 1-35.
- 4 A. Coskun, Chimia, 2020, 74, 667-673.
- 5 Y. Gao, Nanoscale Res. Lett., 2017, 12, 19649-19658.
- 6 L. Wang, Y. Ma, H. Liu, Y. Guo, B. Yang and B. Chang, Sep. Purif. Technol., 2025, 354, 1-13.
- 7 S. G. Stavropoulos, A. Sanida and G. C. Psarras, Appl. Sci., 2021, 11, 7059.
- 8 T. Bertaglia, C. M. Costa, S. Lanceros-Méndez and F. N. Crespilho, Mater. Adv., 2024, 5, 7534-7547.
- 9 T. Bertaglia, C. M. Costa, S. Lanceros-Méndez and F. N. Crespilho, Mater. Adv., 2024, 5, 7534-7547.
- 10 A. Thakur and P. Devi, *Nano Energy*, 2022, **94**, 1-26.
- 11 A. Thakur and P. Devi, Nano Energy, 2022, 94, 1-26.
- 12 X. Jian, S. Liu, Y. Gao, W. Tian, Z. Jiang, X. Xiao, H. Tang and L. Yin, J. Electr. Eng., 2016, 4, 75-87.
- 13 M. Sarno, R. Castaldo, E. Ponticoryo, D. Scarpa, M. Cocca, V. Ambrogi and G. Gentile, Chem. Eng., 2019, 73, 121.
- 14 S. C. Gorgulu, I. Yazar and T. H. Karakoc, J. Mechatron., Artif. Intell., Eng., 2024, 1-13.
- 15 A. A, N. N and R. V, Electrochim. Acta, 2025, 509, 1-10.
- 16 P. Jasrotia and T. Kumar, Structural, electrical, and optical properties of guar gum-based Mg2+ ion conducting biopolymer blend electrolytes, 2024, pp. 139-162.
- 17 P. Jasrotia and T. Kumar, 2024, pp. 139-162.
- 18 J. Sun, B. Luo and H. Li, Adv. Energy Sustainability Res., 2022, 3, 1-26.
- 19 M. Libber, N. Gariya and M. Kumar, J. Solid State Electrochem., 2024, 124, 1-15.
- 20 K. O. Oyedotun and B. B. Mamba, Inorg. Chem. Commun., 2024, 170, 1-18.
- 21 D. R. Lobato-Peralta, P. U. Okoye and C. Alegre, J. Power Sources, 2024, 617, 1-35.
- 22 J. Wen, D. Zhao and C. Zhang, Renewable Energy, 2020, 162, 1629-1648.
- 23 J. Yan, Q. Wang, T. Wei and Z. Fan, Adv. Energy Mater., 2014, 4, 1-43.
- 24 R. T. Yadlapalli, R. R. Alla, R. Kandipati and A. Kotapati, J. Energy Storage, 2022, 49, 1-21.
- 25 S. V. Sadavar, S. Lee and S. Park, Advanced Science, 2024, 1-
- 26 T. Prasankumar, K. Manoharan, N. K. Farhana, S. Bashir, K. Ramesh, S. Ramesh and V. K. Ramachandaramurthy, Mater. Today Sustain., 2024, 28, 1-25.
- 27 H. Du, Z. Wu, Y. Xu, S. Liu and H. Yang, Polymers, 2020, 12,
- 28 V. C. Lokhande, A. C. Lokhande, C. D. Lokhande, J. H. Kim and T. Ji, J. Alloys Compd., 2016, 682, 381-403.
- 29 L. Fu, Q. Qu, R. Holze, V. V. Kondratiev and Y. Wu, J. Mater. Chem. A, 2019, 7, 14937-14970.
- 30 N. S. Shaikh, S. B. Ubale, V. J. Mane, J. S. Shaikh, V. C. Lokhande, S. Praserthdam, C. D. Lokhande and P. Kanjanaboos, J. Alloys Compd., 2022, 893, 1-21.

31 Y. Ma, X. Xie, W. Yang, Z. Yu, X. Sun, Y. Zhang, X. Yang, H. Kimura, C. Hou, Z. Guo and W. Du, Adv. Compos.

- Hybrid Mater., 2021, 4, 906–924.

 32 T. Gupta, Carbon, Springer International Publishing, Cham,
- 33 A. L. Mohamed, H. Gaffer and M. F. Elmansy, *J. Text. Color. Polym. Sci.*, 2024, 21, 239–245.
- 34 D. Datta, V. Colaco, S. P. Bandi, H. Sharma, N. Dhas and P. S. Giram, in *Polymers for Oral Drug Delivery Technologies*, Elsevier, 2025, pp. 263–333.
- 35 A. Sanida, S. G. Stavropoulos, T. Speliotis and G. C. Psarras, J. Therm. Anal. Calorim., 2020, 142, 1701–1708.
- 36 I. O. Oladele, T. F. Omotosho and A. A. Adediran, *Int. J. Polym. Sci.*, 2020, 2020, 8834518.
- 37 A. Al Rashid, S. A. Khan, S. G. Al-Ghamdi and M. Koç, *J. Mater. Res. Technol.*, 2021, **14**, 910–941.
- 38 I. O. Oladele, T. F. Omotosho, G. S. Ogunwande and F. A. Owa, *ppl. Sci. Eng. Prog.*, 2021, **14**, 553–579.
- 39 I. O. Oladele, L. N. Onuh, S. Siengchin, M. R. Sanjay and S. O. Adelani, ppl. Sci. Eng. Prog., 2023, 17, 1–35.
- 40 S. Chandra, D. Uniyal and F. S. Gill, *Journal of Graphic Era University*, 2018, 246–262.
- 41 S. Chen, A. Skordos and V. K. Thakur, *Mater. Today Chem.*, 2020, 17, 100304.
- 42 P. Arunachalam, in *Polymer-based Nanocomposites for Energy and Environmental Applications*, Elsevier, 2018, pp. 185–203.
- 43 K. Rogdakis, N. Karakostas and E. Kymakis, *Energy Environ. Sci.*, 2021, 14, 3352–3392.
- 44 J. Baxter, Z. Bian, G. Chen, D. Danielson, M. S. Dresselhaus, A. G. Fedorov, T. S. Fisher, C. W. Jones, E. Maginn, U. Kortshagen, A. Manthiram, A. Nozik, D. R. Rolison, T. Sands, L. Shi, D. Sholl and Y. Wu, *Energy Environ. Sci.*, 2009, 2, 559–588.
- 45 H. Luo, X. Zhou, C. Ellingford, Y. Zhang, S. Chen, K. Zhou, D. Zhang, C. R. Bowen and C. Wan, *Chem. Soc. Rev.*, 2019, 48, 4424–4465.
- 46 N. Lingappan, S. Lim, G.-H. Lee, H. T. Tung, V. H. Luan and W. Lee, Funct. Compos. Struct., 2022, 4, 1–24.
- 47 A. Hayat, M. Sohail, U. Anwar, T. A. Taha, H. I. A. Qazi, A. S. Amina, Z. Ajmal, A. G. Al-Sehemi, H. Algarni, A. A. Al-Ghamdi, M. A. Amin, A. Palamanit, W. I. Nawawi, E. F. Newair and Y. Orooji, *Chem. Rec.*, 2023, 23, 1–91.
- 48 Z. Ajmal, A. Qadeer, U. Khan, M. Bilal Hussain, M. Irfan, R. Mehmood, M. Abid, R. Djellabi, A. Kumar, H. Ali, A. Kalam, A. G. Al-Sehemi, H. Algarni, Y. Al-Hadeethi, J. Qian, A. Hayat and H. Zeng, *Mater. Today Chem.*, 2023, 27, 1–65.
- 49 Z. Ajmal, M. ul Haq, Y. Naciri, R. Djellabi, N. Hassan, S. Zaman, A. Murtaza, A. Kumar, A. G. Al-Sehemi, H. Algarni, O. A. Al-Hartomy, R. Dong, A. Hayat and A. Qadeer, *Chemosphere*, 2022, 308, 1–16.
- 50 A. Hayat, J. A. Shah Syed, A. G. Al-Sehemi, K. S. El-Nasser, T. A. Taha, A. A. Al-Ghamdi, M. A. Amin, Z. Ajmal, W. Iqbal, A. Palamanit, D. I. Medina, W. I. Nawawi and M. Sohail, *Int. J. Hydrogen Energy*, 2022, 47, 10837–10867.
- 51 I. Hargittai, Struct. Chem., 2024, 35, 1663-1679.

- 52 A. Qadir, S. Shafique, T. Iqbal, H. Ali, L. Xin, S. Ruibing, T. Shi, H. Xu, Y. Wang and Z. Hu, *Sens. Actuators, A*, 2024, 370, 1–27.
- 53 Q. Yang, A. Vriza, C. A. Castro Rubio, H. Chan, Y. Wu and J. Xu, *Chem. Mater.*, 2024, **36**, 2602–2622.
- 54 I. Hargittai, Struct. Chem., 2024, 35, 1663-1679.
- 55 J. Aerathupalathu Janardhanan and H. Yu, *Nanoscale*, 2024, **16**, 17202–17229.
- 56 C. O. Baker, X. Huang, W. Nelson and R. B. Kaner, *Chem. Soc. Rev.*, 2017, 46, 1510–1525.
- 57 Y. Xu, Y. Wang, J. Liang, Y. Huang, Y. Ma, X. Wan and Y. Chen, *Nano Res.*, 2009, 2, 343–348.
- 58 H. A. Abdul Bashid, H. N. Lim, S. Kamaruzaman, S. Abdul Rashid, R. Yunus, N. M. Huang, C. Y. Yin, M. M. Rahman, M. Altarawneh and Z. T. Jiang, *Nanoscale Res. Lett.*, 2017, 12, 1–10.
- 59 F. Wolfart, B. M. Hryniewicz, M. S. Góes, C. M. Corrêa, R. Torresi, M. A. O. S. Minadeo, S. I. Córdoba de Torresi, R. D. Oliveira, L. F. Marchesi and M. Vidotti, *J. Solid State Electrochem.*, 2017, 21, 2489–2515.
- 60 Z. Zhao, K. Xia, Y. Hou, Q. Zhang, Z. Ye and J. Lu, Chem. Soc. Rev., 2021, 50, 12702–12743.
- 61 I. Jeerapan and S. Poorahong, *J. Electrochem. Soc.*, 2020, **167**, 1–19.
- 62 S. J. Varma, K. Sambath Kumar, S. Seal, S. Rajaraman and J. Thomas, *Advanced Science*, 2018, 5, 1–32.
- 63 W. Fu, K. Turcheniuk, O. Naumov, R. Mysyk, F. Wang, M. Liu, D. Kim, X. Ren, A. Magasinski, M. Yu, X. Feng, Z. L. Wang and G. Yushin, *Mater. Today*, 2021, 48, 176–197.
- 64 Z. Zhang, M. Liao, H. Lou, Y. Hu, X. Sun and H. Peng, *Adv. Mater.*, 2018, **30**, 1–19.
- 65 A. A. Ensafi, K. Z. Mousaabadi and R. Fazel-Zarandi, in Conductive Polymers in Analytical Chemistry, ed. A. Amiri and C. M. Hussain, American Chemical Society, Washington, DC, 2022, vol. 1405, pp. 185–217.
- 66 G. Akande, S. A. Ajayi, M. A. Fajobi, O. O. Oluwole and O. S. I. Fayomi, *Key Eng. Mater.*, 2021, 886, 12–29.
- 67 P. Sengodu and A. D. Deshmukh, RSC Adv., 2015, 5, 42109–42130.
- 68 Y. Shi, L. Peng, Y. Ding, Y. Zhao and G. Yu, *Chem. Soc. Rev.*, 2015, 44, 6684–6696.
- 69 M. H. Naveen, N. G. Gurudatt and Y.-B. Shim, *Appl. Mater. Today*, 2017, **9**, 419–433.
- 70 Z.-Q. Hao, J.-P. Cao, Y. Wu, X.-Y. Zhao, Q.-Q. Zhuang, X.-Y. Wang and X.-Y. Wei, *J. Power Sources*, 2017, 361, 249–258.
- 71 Y. N. Sudhakar, M. Selvakumar and D. K. Bhat, *J. Mater. Environ. Sci.*, 2015, **6**, 1218–1227.
- 72 Q. Li, M. Horn, Y. Wang, J. MacLeod, N. Motta and J. Liu, *Materials*, 2019, 12, 703.
- 73 L. Kouchachvili, W. Yaïci and E. Entchev, *J. Power Sources*, 2018, 374, 237–248.
- 74 A. Kausar, Am. J. Phys., 2020, 4, 1-8.
- 75 S. Bhoyate, K. Mensah-Darkwa, P. K. Kahol and R. K. Gupta, *Current Graphene Science*, 2017, 1, 26–43.
- 76 B. Balli, A. Şavk and F. Şen, in *Nanocarbon and its Composites*, Elsevier, 2019, pp. 123–151.

77 S. S. Siwal, Q. Zhang, N. Devi and V. K. Thakur, *Polymers*, 2020, 12, 1–30.

RSC Advances

- 78 J. Wang, S. Dong, B. Ding, Y. Wang, X. Hao, H. Dou, Y. Xia and X. Zhang, *Natl. Sci. Rev.*, 2017, 4, 71–90.
- 79 Q. Li, M. Horn, Y. Wang, J. MacLeod, N. Motta and J. Liu, *Materials*, 2019, **12**, 1–30.
- 80 L. Lyu, H. Chai, K. Seong, C. Lee, J. Kang, W. Zhang and Y. Piao, *Electrochim. Acta*, 2018, 291, 256–266.
- 81 J. Lin, H. Jia, H. Liang, S. Chen, Y. Cai, J. Qi, C. Qu, J. Cao, W. Fei and J. Feng, *Adv. Sci.*, 2018, 5, 1700687.
- 82 J. Jose, V. Thomas, V. Vinod, R. Abraham and S. Abraham, *J. Sci.:Adv. Mater. Devices*, 2019, 4, 333–340.
- 83 M. M. Pérez-Madrigal, M. G. Edo and C. Alemán, *Green Chem.*, 2016, **18**, 5930–5956.
- 84 Y. El-Ghoul, F. M. Alminderej, F. M. Alsubaie, R. Alrasheed and N. H. Almousa, *Polymers*, 2021, 13, 4327.
- 85 B. G. Soares, G. M. O. Barra and T. Indrusiak, *J. Compos. Sci.*, 2021, 5, 173.
- 86 Y.-S. Sung and L.-Y. Lin, Nanomaterials, 2020, 10, 248.
- 87 D. Khokhar, S. Jadoun, R. Arif and S. Jabin, *Polym.-Plast. Technol. Mater.*, 2021, **60**, 465–487.
- 88 S. B. Aziz, M. M. Nofal, R. T. Abdulwahid, H. O. Ghareeb, E. M. A. Dannoun, R. M. Abdullah, M. H. Hamsan and M. F. Z. Kadir, *Polymers*, 2021, **13**, 803.
- 89 S. Sharma, P. Sudhakara, A. A. B. Omran, J. Singh and R. A. Ilyas, *Polymers*, 2021, 13, 2898.
- 90 J. Yang, Q. Cao, X. Tang, J. Du, T. Yu, X. Xu, D. Cai, C. Guan and W. Huang, *J. Mater. Chem. A*, 2021, **9**, 19649–19658.
- 91 S. Y. Liew, D. A. Walsh and G. Z. Chen, *Conducting Polymer Hybrids*, 2017, 269–304.
- 92 Z. Roohi, F. Mighri and Z. Zhang, Multidisciplinary Digital Publishing Institute (MDPI), Conductive Polymer-Based Electrodes and Supercapacitors: Materials, Electrolytes, and Characterizations, 2024, preprint, DOI: 10.3390/ma17164126.
- 93 Z. Genene, Z. Xia, G. Yang, W. Mammo and E. Wang, Recent Advances in the Synthesis of Conjugated Polymers for Supercapacitors, John Wiley and Sons Inc, 2024, DOI: 10.1002/admt.202300167.
- 94 S. Dhibar and C. K. Das, *Ind. Eng. Chem. Res.*, 2014, 53, 3495–3508.
- 95 J. Islam, F. I. Chowdhury, W. Raza, X. Qi, M. R. Rahman, J. Das, J. Uddin and H. M. Zabed, *Renewable Sustainable Energy Rev.*, 2021, 148, 111302.
- 96 R. G. Shrestha, S. Maji, L. K. Shrestha and K. Ariga, *Nanomaterials*, 2020, **10**, 639.
- 97 S. Chen, B. Liu, X. Zhang, F. Chen, H. Shi, C. Hu and J. Chen, *Electrochim. Acta*, 2019, **300**, 373–379.
- 98 C. Sun, Y. Wang, M. D. McMurtrey, N. D. Jerred, F. Liou and J. Li, *Appl. Energy*, 2021, 282, 116041.
- 99 M. Masood, S. Hussain, M. Sohail, A. Rehman, M. A. Uzzaman, I. A. Alnaser, M. R. Karim and Md. A. Wahab, *ChemistrySelect*, 2024, 9, 1–22.
- 100 J.-W. Zha, F. Wang and B. Wan, *Prog. Mater. Sci.*, 2025, **148**, 1–42
- 101 T. Nezakati, A. Seifalian, A. Tan and A. M. Seifalian, *Chem. Rev.*, 2018, **118**, 6766–6843.

- 102 M. Padmini, P. Elumalai and P. Thomas, *Electrochim. Acta*, 2018, 292, 558–567.
- 103 S. Noh, H. Y. Gong, H. J. Lee and W.-G. Koh, *Materials*, 2021, 14, 1-13.
- 104 X. Cai, K. Sun, Y. Qiu and X. Jiao, Crystals, 2021, 11, 1-16.
- 105 M. Shahadat, M. Z. Khan, P. F. Rupani, A. Embrandiri, S. Sultana, S. Z. Ahammad, S. Wazed Ali and T. R. Sreekrishnan, Adv. Colloid Interface Sci., 2017, 249, 2–16.
- 106 L. S. B. Upadhyay, S. Rana and N. Kumar, in Advances in Nanotechnology-Based Drug Delivery Systems, Elsevier, 2022, pp. 533-554.
- 107 M. Porramezan and H. Eisazadeh, *Composites, Part B*, 2011, 42, 1980–1986.
- 108 Y. J. Prasutiyo, A. Manaf and M. A. E. Hafizah, J. Phys.: Conf. Ser., 2020, 1442, 012003.
- 109 F. Zhu, D. Wang, Y. Dang, P. Wang, P. Xu, D. Han and Y. Wei, *Small*, 2025, **21**, 1–12.
- 110 S. Ren, X. Pan, Y. Zhang, J. Xu, Z. Liu, X. Zhang, X. Li, X. Gao, Y. Zhong, S. Chen and S. Wang, *Small*, 2024, 20, e2401346.
- 111 J. Lin, K. Karuppasamy, R. Bose, D. Vikraman, S. Alameri, T. Maiyalagan, H.-S. Kim, A. Alfantazi, J. G. Korvink and B. Sharma, *J. Energy Storage*, 2024, **96**, 112605.
- 112 M. S. A. Darwish, M. H. Mostafa and L. M. Al-Harbi, *Int. J. Mol. Sci.*, 2022, 23, 1023.
- 113 A. Al Rashid, S. A. Khan, S. G. Al-Ghamdi and M. Koç, *J. Mater. Res. Technol.*, 2021, **14**, 910–941.
- 114 M. Beygisangchin, S. Abdul Rashid, S. Shafie, A. R. Sadrolhosseini and H. N. Lim, *Polymers*, 2021, 13, 2003.
- 115 S. Goswami, S. Nandy, E. Fortunato and R. Martins, *J. Solid State Chem.*, 2023, 317, 123679.
- 116 A. K. Sharma, Priya and B. S. Kaith, in *Handbook of Polymer* and *Ceramic Nanotechnology*, Springer International Publishing, Cham, 2019, pp. 1–26.
- 117 S. U. Rahman, P. Röse, U. Krewer, S. Bilal and S. Farooq, *Polymers*, 2021, 1–16.
- 118 M. A. A. M. Abdah, N. H. N. Azman, S. Kulandaivalu and Y. Sulaiman, *Mater. Des.*, 2020, **186**, 108199.
- 119 J. Banerjee, K. Dutta, M. A. Kader and S. K. Nayak, *Polym. Adv. Technol.*, 2019, **30**, 1902–1921.
- 120 D. S. K. Rajaguru, K. P. Vidanapathirana and K. S. Perera, *Sri Lankan J. Phys.*, 2021, **22**, 50.
- 121 Q. Meng, K. Cai, Y. Chen and L. Chen, *Nano Energy*, 2017, 36, 268–285.
- 122 T. Yu, P. Zhu, Y. Xiong, H. Chen, S. Kang, H. Luo and S. Guan, *Electrochim. Acta*, 2016, **222**, 12–19.
- 123 S. R. Sivakkumar, W. J. Kim, J.-A. Choi, D. R. MacFarlane, M. Forsyth and D.-W. Kim, *J. Power Sources*, 2007, 171, 1062–1068.
- 124 H. N. Heme, M. S. N. Alif, S. M. S. M. Rahat and S. B. Shuchi, *J. Energy Storage*, 2021, **42**, 1–25.
- 125 P. Liu, J. Yan, Z. Guang, Y. Huang, X. Li and W. Huang, *J. Power Sources*, 2019, **424**, 108–130.
- 126 Z. Xu, Z. Zhang, H. Yin, S. Hou, H. Lin, J. Zhou and S. Zhuo, *RSC Adv.*, 2020, **10**, 3122–3129.

Review

- 127 B. Devadas and T. Imae, ACS Sustain. Chem. Eng., 2018, 6, 127–134.
- 128 M. Shanmugavadivel, V. V. Dhayabaran and M. Subramanian, *Port. Electrochim. Acta*, 2017, 35, 225–232.
- 129 S.-Y. Lee, J.-I. Kim and S.-J. Park, Energy, 2014, 78, 298-303.
- 130 A. Kathalingam, S. Ramesh, H. M. Yadav, J.-H. Choi, H. S. Kim and H.-S. Kim, *J. Alloys Compd.*, 2020, 830, 154734.
- 131 R. Zhuang, Y. Dong, D. Li, R. Liu, S. Zhang, Y. Yu, H. Song, J. Ma, X. Liu and X. Chen, *J. Alloys Compd.*, 2021, **851**, 1–9.
- 132 S. Rajkumar, E. Elanthamilan, J. P. Merlin and A. Sathiyan, *J. Alloys Compd.*, 2021, **874**, 159876.
- 133 L. Ma, L. Su, J. Zhang, D. Zhao, C. Qin, Z. Jin and K. Zhao, *J. Electroanal. Chem.*, 2016, 777, 75–84.
- 134 R. Srinivasan, E. Elaiyappillai, S. Anandaraj, B. kumar Duvaragan and P. M. Johnson, *J. Electroanal. Chem.*, 2020, **861**, 113972.
- 135 S. Palsaniya, H. B. Nemade and A. K. Dasmahapatra, J. Phys. Chem. Solids, 2021, 154, 110081.
- 136 E. Mitchell, J. Candler, F. De Souza, R. K. Gupta, B. K. Gupta and L. F. Dong, *Synth. Met.*, 2015, **199**, 214–218.
- 137 F. Al-Zohbi, F. Ghamouss, B. Schmaltz, M. Abarbri, M. Zaghrioui and F. Tran-Van, *Materials*, 2021, **14**, 1–16.
- 138 S. Chen, B. Liu, X. Zhang, F. Chen, H. Shi, C. Hu and J. Chen, *Electrochim. Acta*, 2019, **300**, 373–379.
- 139 O. Yoruk, Y. Bayrak and M. Ates, *Polym. Bull.*, 2022, 79, 2969–2993.
- 140 A. K. Thakur, R. B. Choudhary, M. Majumder and M. Majhi, *Ionics*, 2018, **24**, 257–268.
- 141 Q. Chen, F. Xie, G. Wang, K. Ge, H. Ren, M. Yan, Q. Wang and H. Bi, *Ionics*, 2021, 27, 4083–4096.
- 142 K. Gholami laelabadi, R. Moradian and I. Manouchehri, *ACS Appl. Energy Mater.*, 2021, 4, 6697–6710.
- 143 M. G. Hosseini, E. Shahryari and P. Yardani Sefidi, *J. Appl. Polym. Sci.*, 2021, **138**, 50976.
- 144 Y. Fan, H. Chen, Y. Li, D. Cui, Z. Fan and C. Xue, *Ceram. Int.*, 2021, 47, 8433–8440.
- 145 M. Majumder, A. K. Thakur, M. Bhushan and D. Mohapatra, *Electrochim. Acta*, 2021, **370**, 137659.
- 146 W.-F. Ji, M. M. M. Ahmed, A. Bibi, Y.-C. Lee and J.-M. Yeh, *Electrochim. Acta*, 2021, **390**, 1–13.
- 147 H. Heydari, M. Abdouss, S. Mazinani, A. M. Bazargan and F. Fatemi, *J. Energy Storage*, 2021, **40**, 102738.
- 148 N. Kim, S. Kee, S. H. Lee, B. H. Lee, Y. H. Kahng, Y. Jo, B. Kim and K. Lee, *Adv. Mater.*, 2014, **26**, 2268–2272.
- 149 E. Cevik, S. T. Gunday, A. Bozkurt, R. Amine and K. Amine, J. Power Sources, 2020, 474, 228544.
- 150 S. Roy, S. Mishra, P. Yogi, S. K. Saxena, P. R. Sagdeo and R. Kumar, *J. Inorg. Organomet. Polym. Mater.*, 2017, 27, 257–263.
- 151 E. N. Zare, T. Agarwal, A. Zarepour, F. Pinelli, A. Zarrabi, F. Rossi, M. Ashrafizadeh, A. Maleki, M.-A. Shahbazi, T. K. Maiti, R. S. Varma, F. R. Tay, M. R. Hamblin, V. Mattoli and P. Makvandi, Appl. Mater. Today, 2021, 24, 101117
- 152 H. Ashassi-Sorkhabi and A. Kazempour, *J. Mol. Liq.*, 2020, **309**, 113085.

- 153 L. Hao, C. Dong and D. Yu, Polymers, 2024, 16, 2233.
- 154 A. Thadathil, H. Pradeep, D. Joshy, Y. A. Ismail and P. Periyat, *Mater. Adv.*, 2022, **3**, 2990–3022.
- 155 A. Dantas de Oliveira and C. Augusto Gonçalves Beatrice, in *Nanocomposites Recent Evolutions*, IntechOpen, 2019.
- 156 A. Rasool, M. Rizwan, A. ur Rehman Qureshi, T. Rasheed and M. Bilal, in *Smart Polymer Nanocomposites*, Elsevier, 2023, pp. 219–240.
- 157 R. Ullah, N. Khan, R. Khattak, M. Khan, M. S. Khan and O. M. Ali, *Polymers*, 2022, 14, 242.
- 158 K. Arshak, V. Velusamy, O. Korostynska, K. Oliwa-Stasiak and C. Adley, *IEEE Sens. J.*, 2009, **9**, 1942–1951.
- 159 B. Yan, Y. Wu and L. Guo, *Polymers*, 2017, 9, 1-20.
- 160 M. Barazandeh and S. H. Kazemi, Sci. Rep., 2022, 12, 4628.
- 161 K. Zhang, J. Xu, X. Zhu, L. Lu, X. Duan, D. Hu, L. Dong, H. Sun, Y. Gao and Y. Wu, J. Electroanal. Chem., 2015, 739, 66–72.
- 162 D. C. Martin, J. Wu, C. M. Shaw, Z. King, S. A. Spanninga, S. Richardson-Burns, J. Hendricks and J. Yang, *Polym. Rev.*, 2010, 50, 340–384.
- 163 J. Wu, *Doctor of Philosophy*, The University of Michigan, 2011.
- 164 A. M. Díez-Pascual, Polymers, 2021, 13, 2445.
- 165 D. C. Martin, J. Wu, C. M. Shaw, Z. King, S. A. Spanninga, S. Richardson-Burns, J. Hendricks and J. Yang, *Polym. Rev.*, 2010, **50**, 340–384.
- 166 A. Elschner, S. Kirchmeyer, W. Lovenich, U. Merker and K. Reuter, PEDOT: Principles and Applications of an Intrinsically Conductive Polymer, CRC press, 2010.
- 167 F. Ahmad, A. Shahzad, S. Sarwar, H. Inam, U. Waqas, D. Pakulski, M. Bielejewski, S. Atiq, S. Amjad, M. Irfan, H. Khalid, M. Adnan and O. Gohar, *J. Power Sources*, 2024, 619, 1–24.
- 168 A. B. Olabintan, A. S. Abdullahi, B. O. Yusuf, S. A. Ganiyu, T. A. Saleh and C. Basheer, *Microchem. J.*, 2024, **204**, 1–21.
- 169 C. Badre, L. Marquant, A. M. Alsayed and L. A. Hough, *Adv. Funct. Mater.*, 2012, **22**, 2723–2727.
- 170 S. Kirchmeyer and K. Reuter, *J. Mater. Chem.*, 2005, **15**, 2077–2088.
- 171 I. Shown, A. Ganguly, L. Chen and K. Chen, *Energy Sci. Eng.*, 2015, 3, 2–26.
- 172 T. S. Sonia, P. A. Mini, R. Nandhini, K. Sujith, B. Avinash, S. V Nair and V. Subramanian, *Composite Supercapacitor Electrodes Made of Activated carbon/PEDOT:PSS and Activated Carbon/doped PEDOT*, 2013, vol. 36.
- 173 T. L. Kelly, K. Yano and M. O. Wolf, *ACS Appl. Mater. Interfaces*, 2009, **1**, 2536–2543.
- 174 F. J. González, A. Montesinos, J. Araujo-Morera, R. Verdejo and M. Hoyos, *J. Compos. Sci.*, 2020, 4, 87.
- 175 R. K. Sharma and L. Zhai, *Electrochim. Acta*, 2009, **54**, 7148–7155.
- 176 S. Khasim, A. Pasha, N. Badi, M. Lakshmi and Y. K. Mishra, *RSC Adv.*, 2020, **10**, 10526–10539.
- 177 V. Kumar, S. Kalia and H. C. Swart, Springer Series on Polymer and Composite Materials Conducting Polymer Hybrids, 2017.
- 178 K. Namsheer and C. S. Rout, RSC Adv., 2021, 11, 5659-5697.

- 179 K. Tõnurist, T. Thomberg, A. Jänes, T. Romann, V. Sammelselg and E. Lust, J. Electroanal. Chem., 2013, **689**, 8-20.
- 180 J. Zhang, M. Gu and X. Chen, Micro Nano Eng., 2023, 21,
- 181 A. M. Bryan, L. M. Santino, Y. Lu, S. Acharya and J. M. D'Arcy, Chem. Mater., 2016, 28, 5989-5998.
- 182 M. E. Abdelhamid, A. P. O'Mullane and G. A. Snook, RSC Adv., 2015, 5, 11611-11626.
- 183 Y. Wang, Y. Shi, L. Pan, Y. Ding, Y. Zhao, Y. Li, Y. Shi and G. Yu, Nano Lett., 2015, 15, 7736-7741.
- 184 S. H. Lee, S. Lee, H. W. Ryu, H. Park, Y. S. Kim and J. H. Kim, J. Polym. Sci., Part A:Polym. Chem., 2014, 52, 2329-2336.
- 185 D. Y. Su, Z. G. Liu, L. Jiang, J. Hao, Z. J. Zhang and J. Ma, in IOP Conference Series: Earth and Environmental Science, Institute of Physics Publishing, 2019, vol. 267.
- 186 M. G. Tadesse, A. S. Ahmmed and J. F. Lübben, Review on conductive polymer composites for supercapacitor applications, Multidisciplinary Digital Publishing Institute (MDPI), 2024, preprint, DOI: 10.3390/jcs8020053.
- 187 A. Chonat, Energy Fuels, 2023, 37, 3555-3569.
- 188 A. Agarwal, R. Tolani and B. R. Sankapal, Conducting Polymers-Metal Chalcogenides Hybrid Composite: Current Trends and Future Prospects toward Supercapacitor Applications, John Wiley and Sons Inc, 2024, DOI: 10.1002/ente.202400133.
- 189 H. Islam and M. E. Hoque, in Advanced Polymer Nanocomposites, Elsevier, 2022, pp. 415-441.
- 190 J. Sarfraz, T. Gulin-Sarfraz, J. Nilsen-Nygaard and M. K. Pettersen, Nanomaterials, 2020, 11, 10.
- 191 C. Vasile, Materials, 2018, 11, 1834.
- 192 Z. Honarvar, Z. Hadian and M. Mashayekh, Electron. Physician, 2016, 8, 2531-2538.
- 193 N. Basavegowda and K.-H. Baek, *Polymers*, 2021, 13, 4198.
- 194 Y. Dang, F. Zhu, D. Wang, S. Yu, Y. Wei and D. Han, Acta Mater., 2025, 284, 120588.
- 195 D. Gao, R. Liu, D. Han, P. Xu, P. Wang and Y. Wei, J. Mater. Chem. A, 2023, 11, 9546-9554.
- 196 F. Zhu, D. Wang, Y. Dang, P. Wang, P. Xu, D. Han and Y. Wei, Small, 2024, 21, 1-12.
- 197 Z. Wang, H. Cui, S. Li, X. Feng, J. Aghassi-Hagmann, S. Azizian and P. A. Levkin, ACS Appl. Mater. Interfaces, 2021, 13, 21661-21668.

- 198 H. Li, Y. Liu, S. Liu, P. Li, C. Zhang and C. He, Composites, Part A, 2023, 166, 107386.
- 199 C. Zhu, H. Xue, H. Zhao, T. Fei, S. Liu, Q. Chen, B. Gao and T. Zhang, Talanta, 2022, 242, 123289.
- 200 B. Dudem, A. R. Mule, H. R. Patnam and J. S. Yu, Nano Energy, 2019, 55, 305-315.
- 201 S. Sun, Y. Xu and X. Maimaitiyiming, React. Funct. Polym., 2023, 190, 105625.
- 202 Md. A. Shahid, Md. M. Rahman, Md. T. Hossain, I. Hossain, Md. S. Sheikh, Md. S. Rahman, N. Uddin, S. W. Donne and Md. I. U. Hoque, J. Compos. Sci., 2025, 9, 42.
- 203 A. Dube, S. J. Malode, A. N. Alodhayb, K. Mondal and N. P. Shetti, Talanta, 2025, 11, 100395.
- 204 L. Manjakkal, L. Pereira, E. Kumi Barimah, P. Grev, F. F. Franco, Z. Lin, G. Jose and R. A. Hogg, Prog. Mater. Sci., 2024, 142, 101244.
- 205 Y. Sun, S. P. Lacour, R. A. Brooks, N. Rushton, J. Fawcett and R. E. Cameron, J. Biomed. Mater. Res., Part A, 2009, 90, 648-655.
- 206 H. M. Saleh and A. I. Hassan, Sustainability, 2023, 15, 10891.
- 207 F. Znidi, M. Morsy and Md. N. Uddin, Heliyon, 2024, 10, e32843.
- 208 Y. Wu, D. Xiao, P. Liu, Q. Liao, Q. Ruan, C. Huang, L. Liu, D. Li, X. Zhang, W. Li, K. Tang, Z. Wu, G. Wang, H. Wang and P. K. Chu, Research, 2023, 6, 0074.
- 209 W. Cheng, Z. Zheng, X. Li, Y. Zhu, S. Zeng, D. Zhao and H. Yu, Research, 2024, 22, 0383.
- 210 Z. Wang and R. Liu, Mater. Today Electron., 2023, 4, 100036.
- 211 M. Sarno, L. Baldino, C. Scudieri, S. Cardea and E. Reverchon, J. Phys. Chem. Solids, 2020, 136, 109132.
- 212 H. Duan, Y. Liu and X. Zhao, Recent research progress of conductive polymer-based supercapacitor electrode materials, SAGE **Publications** Ltd, 2023, 10.1177/ 00405175231167602
- 213 M. Masood, S. Hussain, M. Sohail, A. Rehman, M. A. Uzzaman, I. A. Alnaser, M. R. Karim and M. A. Wahab, Recent progress, challenges, and opportunities of conducting polymers for energy storage applications, John Wiley and Sons Inc, 2024, DOI: 10.1002/slct.202302876.